THE NATURE OF THE DARK MATTER

KIM GRIEST

Physics Department
University of California, San Diego, La Jolla CA 92093

1. Introduction

The dark matter problem has been around for decades, and there is now consensus that we don't know what the most common material in the Universe is [1]. It is "seen" only gravitationally, and does not seem to emit or absorb substantial electromagnetic radiation at any known wavelength. It dominates the gravitational potential on scales from tiny dwarf galaxies, to large spiral galaxies like the Milky Way, to large clusters of galaxies, to the largest scales yet explored. The universal average density of dark matter determines the ultimate fate of the Universe, and it is clear that the amount and nature of dark matter stands as one of the major unsolved puzzles in science.

In this series of talks I will first recall the evidence for dark matter, with emphasis on the dark matter in our own Galaxy. This overlaps somewhat with Primack's lecture [these proceedings], so I will be brief. I then turn to the dark matter candidates and how we might discover which (if any) of them actually exists. Then, I will focus in on two of my favorite candidates, the supersymmetric neutralino Wimp candidate, and the baryonic Macho candidate. For the later candidate, I will go into some detail concerning the one particular experiment with which I am involved, and present some results showing, that over a broad range of masses, this candidate has been ruled out as the primary constituent of the dark matter in our Galaxy. For the supersymmetric Wimp and especially the neutrino and axion candidates I will be brief, since there will be talks by Masiero [these proceedings] on these topics.

⋆ Lectures presented at the International School of Physics "Enrico Fermi" Course "Dark Matter in the Universe", Varenna, 25 July - 4 August, 1995.

2. Physical Evidence for Dark Matter

Evidence for dark matter (DM) exists on many scales, and it is important to remember that the dark matter on different scales may be different – the dark matter in dwarf spirals may not be the dark matter which contributes $\Omega = 1$; in fact, the $\Omega = 1$ dark matter may not exist. This consideration is especially important when discussing dark matter detection, since detection is done in the Milky Way and its environs, and evidence for dark matter outside the Milky Way may not be relevant. So, let me start with an inventory of dark matter in the Universe.

The cosmological density of dark matter on different scales is quoted using $\Omega = \rho/\rho_{crit}$, where ρ is the density of some material averaged over the Universe, and ρ_{crit} is the critical density. Most determinations of Omega are made by measuring the mass-to-light ratio Υ of some system and then multiplying this by the average luminosity density of the Universe: $j_0 = 1.9 \pm 0.1 \times 10^8 h^{-1} L_\odot/M_\odot$ [Kirshner, these proceedings]. Here $h = 0.4-1$ parameterizes our uncertainty of the Hubble constant. There are methods, such as Ω_{baryon} from big bang nucleosynthesis, and potential reconstruction from bulk flows, which do not use depend upon j_0, but methods which involve taking an inventory of material depend upon it. For example, the mass-to-light ratio in the solar neighborhood is $\Upsilon \approx 5$, giving $\Omega_{lum} = 0.003 h^{-1} = 0.003 - 0.007$. If the solar neighborhood is typical, the amount of material in stars, dust and gas is far below the critical value.

2.1 Spiral Galaxies

The most robust evidence for dark matter comes from the rotation curves of spiral galaxies. Using 21 cm emission, the velocities of clouds of neutral hydrogen can be measured as a function of r, the distance from the center of the galaxy. In almost all cases, after a rise near $r = 0$, the velocities remain constant out as far as can be measured. By Newton's law for circular motion $GM(r)/r^2 = v^2/r$, this implies that the density drops like r^{-2} at large radius and that the mass $M(r) \propto r$ at large radii. Once r becomes greater than the extent of the mass, one expects the velocities to drop $\propto r^{-1/2}$, but this is not seen, implying that we do not know how large the extended dark halos around spirals are. For example, the rotation curve of NGC3198 [2] implies $\Upsilon > 30h$, or $\Omega_{halo} > 0.017$. The large discrepancy between this number and Ω_{lum} is seen in many external galaxies and is the strongest evidence for dark matter.

It is fortunate that the most secure evidence for dark matter is in spiral galaxies, since searches for dark matter can be made only in spiral galaxies; in fact only in our spiral, the Milky Way. Unfortunately, the rotation curve of the Milky Way is not well constrained, with recent measurements extending only to 15 to 20 kpc, and having differing amplitudes and shapes [3,4]. This leads to substantial uncertainty in the amount of dark matter in our Galaxy. There are other indicators of the mass

of the Milky Way. By studying the motion of dwarf galaxies (especially Leo I at a distance of 230 kpc) Zaritsky, *et al.* [5] find a mass of the Milky Way of $M_{MW} = 1.25^{+0.8}_{-0.3} \times 10^{12} M_\odot$, for $\Upsilon_{MW} \approx 90$, and $\Omega_{MW} \approx 0.054 h^{-1}$ (assuming the Universe is like the Milky Way). A very recent study by Kochanek [6], does a maximum likelihood analysis including constraints from satellite velocities, the distribution of high velocity stars (local escape velocity), the rotation curve, and the tidal effects of M31, to find a mass of the Milky Way inside 50 kpc of $5.4 \pm 1.3 \times 10^{11} M_\odot$. It is interesting that this value is just what one expects from a flat rotation curve with $v = 220$ km/sec out to 50 kpc, so the Milky Way is very likely a typical spiral with a large dark halo.

2.2 Clusters of Galaxies

Moving to larger scales, the methods of determining Ω become less secure, but give larger values. There is a great deal of new evidence on dark matter in clusters of galaxies, coming from gravitational lensing [7] from X-ray gas temperatures [8] and from the motions of cluster member galaxies. For example, consider the Coma cluster which contains around a thousand galaxies. White *et al.* [9] recently collated some of the data on the Coma cluster, reporting separate measurements of the amount of mass in stars, hot gas, and in total. Within a radius of $1.5 h^{-1}$ Mpc, they give

$$\begin{aligned} M_{star} =& 1.0 \pm 0.2 \times 10^{13} h^{-1} M_\odot \\ M_{gas} =& 5.4 \pm 1 \times 10^{13} h^{-5/2} M_\odot \\ M_{total} =& 5.7 - 11 \times 10^{14} h^{-1} M_\odot, \end{aligned}$$

where the total mass is estimated in two completely different ways. The first method is a refinement of Zwicky's method of using the radial velocities of the member galaxies, and the assumption of virialization to gauge the depth of the gravitational potential well. The second method makes use of the ROSAT X-ray maps and the assumption of a constant temperature equilibrium to get the same information. Remarkably the two methods give the same mass within errors. Thus with a mass-to-light ratio of $\Upsilon = 330 - 620 M_\odot / L_\odot$, one finds $\Omega = 0.2 - 0.4$, if the inner 1.5 Mpc of Coma is representative of the Universe as a whole.

There is, however, a disconcerting in about the above numbers. As pointed out by White, *et al.* [9]

$$\frac{M_{baryon}}{M_{total}} > 0.009 + 0.05 h^{-3/2}.$$

Now the Coma cluster is large enough that one might expect its baryon to dark matter ratio to be the Universal value, ($\Omega_{baryon}/\Omega_{total} = M_{baryon}/M_{total}$), and in fact White, *et al.* argue that this is the case. Then the inequality above should apply

to the entire Universe. But, big bang nucleosynthesis limits $\Omega_{baryon} < 0.015h^{-2}$. If $\Omega_{total} = 1$, the two inequalities are in quite strong disagreement for any value of h. So this is a puzzle. The conclusions of White, *et al.*, are that either Ω is not unity, or that big bang nucleosynthesis is not working. However, there are other possible explanations, notably that the measurements of the total mass in clusters by gravitational lensing tend to give larger total mass than the X-ray and virial methods, and that mass and velocity bias may mean that clusters are not representative of the Universe as a whole. The story is clearly not yet finished.

2.3 Large Scale Flows

It would be best to measure the amount of dark matter on the largest possible scales so that the sample is representative of the entire Universe. Within the past several years a host of large-scale flow methods have been tried and are giving impressive results [10]. These methods have the advantage stated above but the disadvantage that they depend upon assumptions about galaxy formation—that is, they depend upon gravitational instability theory, the assumption of linear biasing, etc. Also, the errors in these measurements are still large and the calculations are complicated, but they do have great promise, and tend to give values of Ω near unity.

A simple example comes from the observation that the local group of galaxies moves at 627 ± 22 km sec^{-1} with respect to the cosmic microwave background (CMB) (measured from the amplitude of the CMB dipole). If this motion comes from gravity, then the direction of the motion should line up with the direction where there is an excess of mass, and the velocity should be determined by the size of this excess. Thus, taking into account the expansion of the Universe, one has

$$v \propto \Omega^{0.6} \frac{\delta\rho}{\rho} = \frac{\Omega^{0.6}}{b} \frac{\delta n}{n},$$

where the linear bias factor b has been introduced to relate the observed excess in galaxy number counts $\delta n/n$ to the excess in mass density $\delta\rho/\rho$. Using galaxy counts from the IRAS satellite survey, Yahil *et al.* [11] find that the direction of the $\delta n/n$ excess agrees with the direction of the velocity vector to within $\sim 20^0$, and that

$$\beta \equiv \frac{\Omega^{0.6}}{b} = 0.9 \pm 0.2.$$

Thus with the very conservative limit $b > 0.5$, one has $\Omega > 0.2$, and with the reasonable limit $b > 1$, one finds $\Omega > 0.5$. For this method to be reliable, $\delta n/n$ must be measured on very large scales to ensure that convergence has been reached, and it is not sure that this is the case.

The above technique is only one of many related methods used to determine Ω on large scales. Another example is the detailed comparison of the peculiar velocities of many galaxies with the detailed maps of $\delta n/n$. This should not only determine Ω, but serve as a stringent test for the theory that large-scale structure is formed by gravitational instability. A recent review by Dekel [10] surveys many such methods and concludes that reasonable evidence exists for $\Omega > 0.3$. Although these techniques holds much promise, it should be noted that different analyses of the same data sometimes lead to different conclusions. So for the time being, these estimates of β should not yet be viewed as robust [12].

In conclusion, the observational evidence for large amounts of dark matter on galactic halo scales is overwhelming. On larger scales, the observational evidence for Ω in the 0.1 to 0.2 range is strong. On the largest scales, substantial observational evidence exists for $\Omega > 0.3$, and some evidence for Ω near unity exists, although this may be in conflict with observations on cluster scales.

2.4 The Baryonic Content of the Universe

An important ingredient in the motivation for non-baryonic dark matter comes from big-bang-nucleosynthesis limits on the average baryonic content of the Universe. To agree with the measured abundances of helium, deuterium, and lithium, the baryonic content of the Universe must be between $0.01 < \Omega_b h^2 < 0.015$ [13,14,15]. Given the large uncertainty in h this means $0.01 < \Omega_b < 0.1$. These values are far below unity, so the theoretical predilection for $\Omega_{total} = 1$ (or the observational evidence for $\Omega > 0.3$) forces the bulk of the dark matter to be non-baryonic. The lower limit of this range is actually *above* the abundance of known stars, gas, etc., and so there also seems to be evidence for substantial *baryonic* dark matter as well.

However, if one considered only the most secure dark matter, that found in spiral galaxies, then it is completely possible that it is all baryonic. Since this is the only dark matter which is directly accessible to experimental detection, it is crucial to consider the possibility of an entirely baryonic dark halo.

2.5 Distribution of Dark Matter in the Milky Way

While we don't know what the dark matter (DM) is, we have a fairly reasonable idea as to how much of it there is in the Galaxy, how it is distributed, and how fast it is moving. This information comes from the rotation curve of the Milky Way, and is crucial to all the direct searches for dark matter. If we say that the rotation curve of the Milky Way is constant at about $v_c = 220$ km/sec out to as far as it is measured, then we know that the density must drop as r^{-2} at large distances. This velocity also sets the scale for the depth of the potential well and says that the dark matter must also move with velocities in this range. Assuming a spherical

and isotropic velocity distribution is common, and a usual parameterization is

$$\rho(\mathbf{r}) = \rho_0 \frac{a^2 + r_0^2}{a^2 + r^2},$$

where $r_0 \approx 8.5$ kpc is the distance of the Sun from the galactic center, a is the core radius of the halo, and $\rho_0 \approx 0.3$ GeV cm^{-3} is the density of dark matter near the Sun. Also, a typical velocity distribution is

$$f(v)d^3v = \frac{e^{-v^2/v_c^2}}{\pi^{3/2}v_c^3} d^3v.$$

It should be noted that the specifics of the above models are not very secure. For example, it is quite possible that the halo of our Galaxy is flattened into an ellipsoid, and there may be a component of the halo velocity which is rotational and not isotropic. Also, some (or even most) of the rotation curve of the Milky Way at the solar radius could be due to the stellar disk. Canonical models of the disk have the disk contributing about half the rotation velocity, but larger disks have been envisioned. Recent microlensing results may be indicative of a larger disk as well (see Section 7.).

Finally, other important points about our Galaxy's geography include the fact that the nearest two galaxies are the LMC and SMC, located at a distance of 50 kpc and 60 kpc respectively, that the halo of the Milky Way is thought to extend out at least this far, and that the bulge of the Milky Way is a concentration of stars in the center of our Galaxy (8.5 kpc away) with a size of about 1 kpc.

3. Brief Survey of Dark Matter Candidates

There is no shortage of ideas as to what the dark matter could be. In fact, the problem is the opposite. Serious candidates have been proposed with masses ranging from 10^{-5} eV $= 1.8 \times 10^{-41}$ kg $= 9 \times 10^{-72} M_\odot$ (axions) up to $10^4 M_\odot$ black holes. That's a range of masses of over 75 orders of magnitude! It should be clear that no one search technique could be used for all dark matter candidates.

Even finding a consistent categorization scheme is difficult, so we will try a few. First, as discussed above, is the baryonic vs non-baryonic distinction. The main baryonic candidates are the Massive Compact Halo Object (Macho) class of candidates. These include brown dwarf stars, jupiters, and 100 $M_\odot$ black holes. Brown dwarfs are spheres of H and He with masses below 0.08 $M_\odot$, so they never begin nuclear fusion of hydrogen. Jupiters are similar but with masses near 0.001 $M_\odot$. Black holes with masses near 100 $M_\odot$ could be the remnants of an early generation of stars which were massive enough so that not many heavy elements were dispersed

when they underwent their supernova explosions. Other, less popular, baryonic possibilities include fractal or specially placed clouds of molecular hydrogen [16]. The non-baryonic candidates are basically elementary particles which are either not yet discovered or have non-standard properties. Outside the baryonic/non-baryonic categories are two other possibilities which don't get much attention, but which I think should be kept in mind until the nature of the dark matter is discovered. The first is non-Newtonian gravity. See Begeman *et al.* [17] for a provocative discussion of this possibility; but watch for results from gravitational lensing which may place very strong constraints. Second, we shouldn't ignore the "none-of-the-above" possibility which has surprised the Physics/Astronomy community several times in the past.

Among the non-baryonic candidates there are several classes of particles which are distinguished by how they came to exist in large quantity during the Early Universe, and also how they are most easily detected. The axion (Section 5) is motivated as a possible solution to the strong CP problem and is in a class by itself. The largest class is the Weakly Interacting Massive Particle (Wimp) class (Sections 4 and 6), which consists of literally hundreds of suggested particles. The most popular of these Wimps is the neutralino from supersymmetry (Section 6). Finally, if the tau and/or muon neutrino had a mass in the 2 eV to 100 eV range, they could make up all or a portion of the dark matter. This possibility will be discussed by Masiero and also Klypin [these proceedings].

Another important categorization scheme is the "hot" vs "cold" classification. A dark matter candidate is called "hot" if it was moving at relativistic speeds at the time when galaxies could just start to form (when the horizon first contained about $10^{12} M_{\odot}$). It is called "cold" if it was moving non-relativistically at that time. This categorization has important ramifications for structure formation, and there is a chance of determining whether the dark matter is hot or cold from studies of galaxy formation. Hot dark matter cannot cluster on galaxy scales until it has cooled to non-relativistic speeds, and so gives rise to a considerably different primordial fluctuation spectrum [see Klypin, these proceedings]. Of the above candidates only the light neutrinos would be hot; all the others would be cold.

4. Thermal Relics as Dark Matter (Wimps)

Among the particle dark matter candidates an important distinction is whether the particles were created thermally in the Early Universe, or whether they were created non-thermally in a phase transition. Thermal and non-thermal relics have a different relationship between their relic abundance Ω and their properties such as mass and couplings, so the distinction is especially important for dark matter detection efforts. For example, the Wimp class of particles can be defined as those particles which are created thermally, while dark matter axions come mostly from non-thermal processes.

In thermal creation one imagines that early on, when the Universe was at very high temperature, thermal equilibrium obtained, and the number density of Wimps (or any other particle species) was roughly equal to the number density of photons. As the Universe cooled the number of Wimps and photons would decrease together as long as the temperature remained higher than the Wimp mass. When the temperature finally dropped below the Wimp mass, creation of Wimps would require being on the tail of the thermal distribution, so in equilibrium, the number density of Wimps would drop exponentially $\propto \exp(-m_{Wimp}/T)$. If equilibrium were maintained until today there would be very few Wimps left, but at some point the Wimp density would drop low enough that the probability of one Wimp finding another to annihilate would become small. (Remember we must assume that an individual Wimp is stable if it is to become the dark matter.) The Wimp number density would "freeze-out" at this point and we would be left with a substantial number of Wimps today. Detailed evolution of the Boltzmann equation can be done for an accurate prediction [Section 6.2], but roughly

$$\Omega_{Wimp} \approx \frac{10^{-26}\mathrm{cm}^3\mathrm{s}^{-1}}{\langle \sigma v \rangle},$$

where $\langle \sigma v \rangle$ is the thermally averaged cross section for two Wimps to annihilate into ordinary particles. The remarkable fact is that for $\Omega \approx 1$, as required by the dark matter problem, the annihilation cross section $\langle \sigma v \rangle$ for any thermally created particle turns out to be just what would be predicted for particles with electroweak scale interactions. Thus the "W" in "Wimp". There are several theoretical problems with the Standard Model of particle physics which are solved by new electroweak scale physics such as supersymmetry. Thus these theoretical problems may be clues that the dark matter does indeed consist of Wimps. Said another way, any stable particle which annihilates with an electroweak scale cross section is bound to contribute to the dark matter of the Universe. It is interesting that theories such as supersymmetry, invented for entirely different reasons, typically predict just such a particle.

The fact that thermally created dark matter has weak scale interactions also means that it may be within reach of accelerators such as LEP at CERN, and CDF at Fermilab. After all these accelerators were built precisely to probe the electroweak scale. Thus many accelerator searches for exotic particles are also searches for the dark matter of the Universe. Also, due to the weak scale interactions, Wimp-nuclear interaction rates are within reach of many direct and indirect detection methods (see Section 6).

5. Non-thermal Relics as Dark Matter (Axions)

The best example of a non-thermal particle dark matter candidate is the axion [18]. Actually, thermal axions are produced in the standard way, but if such axions existed in numbers so as to make up the dark matter, they would have lifetimes too short to still be around in quantity. However, there is another, more important, production mechanism for axions in the early Universe.

The axion arises because the QCD Lagrangian contains a term

$$L \supset \frac{\bar{\theta} g^2}{32\pi^2} G\tilde{G},$$

where G is the gluon field strength. This term predicts an electric dipole moment of the neutron of is $d_n \approx 5 \times 10^{-16}\bar{\theta}$. Experimentally, however, the neutron dipole moment $d_n < 10^{-25}$, which means $\bar{\theta} < 10^{-10}$. The question is why does this $\bar{\theta}$ parameter have such a small value, when it naturally would have a value near unity? This is the strong CP problem, and one way to resolve this problem is to introduce a new Peccei-Quinn symmetry which predicts a new particle – the axion. The P-Q symmetry forces $\bar{\theta} = 0$ at low temperatures today, but in the early Universe, the axion field was free to roll around the bottom of its Mexican hat potential. The axion field motion in the angular direction is called θ, and since the curvature of the potential in this direction is zero, the axion at high temperatures was massless. However, when the temperature of the Universe cooled below a few hundred MeV (QCD energy scale), the axion potential "tilts" due to QCD instanton effects, and the axion begins to oscillate around the minimum, like a marble in the rim of a tilted Mexican hat. The minimum of the potential forces the average $\bar{\theta}$ to zero, solving the strong CP problem, and the curvature of the potential means the axion now has a mass. There is no damping mechanism for the axion oscillations, so the energy density which goes into oscillation remains until today as a coherent axion field condensate filling the Universe. This is a zero momentum condensate and so constitutes cold dark matter. One can identify this energy density as a bunch of axion particles, which later can become the dark matter in halos of galaxies. The relic energy density Ω is thus related to the tilt of the potential, which in turn is related to the axion mass, a free parameter of the model. If the axion mass $m_a \approx 10^{-5}$ eV, then $\Omega_a \approx 1$. One now sees why axions are cold dark matter even though they are so light. This rather unusual story is probably the most elegant solution to the strong CP problem, and several groups are mounting laboratory searches for the coherent axions which may make up the major component of mass in the Galaxy. For example, a group involving physicists from Lawrence Livermore National Lab, the Russian INR, the University of Florida, MIT, Fermilab, UC Berkeley, LBL, and the University of Chicago [19] is building an extremely loise noise microwave cavity inside of a large magnetic field for this purpose. The basic idea is that halo axions can interact with the magnetic field and produce microwave photons. This will happen resonantly when the cavity is tuned precisely to the axion

mass, so one scans the frequency spectrum looking for such a resonance signal. Two experiments, one at Florida and one at Brookhaven have already used this technique and reported negative results [20]. The sensitivity of thoses early experiments was significantly below the expected signal, however, and it is this new experiment which will for the first time have the capability of detecting dark matter axions if in fact they exist.

6. Search for Wimp Dark Matter (Neutralinos)

Why is it important to actually search for and to identify the dark matter? Of course it is intrinsically interesting to know what the primary constituent of the Universe consists of, but also until we know the dark matter identity, there will always be the doubt that there is no dark matter, and instead there is some flaw in our knowledge of fundamental physics.

Unfortunately, no one technique is useful for all the different candidates. The only way to proceed is to pick a candidate and design an experiment specific to that candidate. This is risky proposition, especially for the experimentalist who must spend many years of his or her life developing the technology and performing the search. For this reason, only the best motivated candidates are currently being searched for. There are hundreds of other dark matter candidates that we have not discussed at all. As one goes down the list of popular candidates, asking oneself which candidate is the most likely, I have to admit that "none-of-the-above" comes to mind. However, it is difficult to make any progress searching for an unspecified candidate. After "none-of-the-above", I think the Wimp candidates, and especially the supersymmetric neutralino candidate, is probably the best bet. It may sound odd to an astrophysically oriented group such as yourselves that my best guess for the dark matter is a specific undiscovered elementary particle based on a theory for which there is no evidence, so I will spend some time describing my somewhat idiosyncratic reasons.

Please see the lectures by A. Masiero [these proceedings] for additional in depth discussion of many of the issues covered here. Also see the new Physics Report "Supersymmetric Dark Matter", by Jungman, Kamionkowski, and myself for more details on everything covered here.

6.1 Motivation for Supersymmetry

First, why should astrophysicists take seriously supersymmetry, a theory which requires more than doubling the number of known elementary particles, none of which has yet been detected? When Dirac attempted to make special relativity consistent with quantum mechanics he discovered the Dirac equation. He also discover a disconcerting fact. There was a new symmetry, CPT symmetry, implied

by his equation, and this symmetry required that for every known particle there had exist a charge conjugate, or anti-particle. He resisted the idea of doubling the number of known particles, and initially hypothesized that the CPT partner of the electron was the proton. This idea was soon shown to be impossible, but fortunately the anti-electron and anti-proton were soon discovered, vindicating Dirac's theory.

The situation may be similar with regard to supersymmetry. Many attempts have been made to make general relativity consistent with quantum field theory, especially within the framework of a theory which combines gravity with the strong and electroweak interactions. It is interesting that in all the most successful attempts a new symmetry is required. The powerful Coleman-Mandula theorem states that within the framework of Lie algebras, there is no way to unify gravity with the gauge symmetries which describe the strong and electroweak interactions. So the "super"-symmetry which successfully combines these interactions had to move beyond Lie algebras to "graded" Lie algebras. Graded Lie algebras are just like Lie algebras except they use anti-commutation relations instead of commutation relations. Thus they relate particles with spin particles to without spin. Examples of theories that attempt to combine gravity with the other forces include superstrings and super-gravity, where in both cases "super" refers to the supersymmetry. Thus, if such a symmetry exists in nature, every particle with spin (fermion) must have a related super-symmetric partner without spin (boson), and vice versa. As it now stands, standard quantum field theory seems to be incompatible with general relativity. Since the world is unlikely to be incompatible with itself, it seems either quantum field theory or general relativity must be modified, and of course a new theory which combines gravity with the strong and electroweak interactions would be the most elegant. Thus, one sees why so many particle physicists have become enamored with supersymmetry, and why many thousands of papers have been written on the subject.

As in Dirac's case, this doubling of the number of particles was disconcerting, and it was initially hoped that perhaps the neutrino could be supersymmetric partner of the photon. Now it is known that this is impossible, but unlike in Dirac's case, no discovery of supersymmetric partners has quickly followed. In fact, it is now known that supersymmetry must be a "broken" symmetry, since perfect supersymmetry requires that the masses of the super-partners be the same as their counterparts. This is easily arranged, but leaves the masses of all the superpartners undetermined. In fact, the masses could be so large that all the superpartners are completely undetectable in current or future accelerators and are therefore mostly irrelevant to current physics or dark matter detection. There are however some very suggestive reasons why the superpartners may have masses in the 100 GeV to several TeV range.

First, there is coupling constant unification. The strength of the strong, weak, and electromagnetic interactions is set by the value their coupling constants, and

these "constants" change as the energy of the interactions increase. For example, the electromagnetic coupling constant $\alpha = \frac{1}{137}$, has a value near $\frac{1}{128}$ when electrons are collided at the LEP machine at CERN. Several decades ago it was noticed that the three coupling constants would meet together at a universal value when the energy of interactions reached about 10^{15} GeV. This would allow a "Grand Unification" of the strong, weak, and electromagnetic interactions, and much model building was done. In the past few years, the values of the three coupling constants have been measured much more accurately, and it is now clear that, in fact, they cannot unify at any scale unless many new particles are added to the theory. Suggestively, if the supersymmetric partners exist, and have reasonably low masses they give just the right contribution to force the coupling constants to unify.

Next, there is the gauge hierarchy problem. The standard model of particle physics is enormously successful. It accurately predicts the results of hundreds of measurements. In the standard model, fermions such as electrons are intrinsically massless, but develop a mass through interactions with the Higgs field that is hypothesized to fill the Universe. The mass of a fermion then is just proportional to the strength of its coupling to the Higgs field. The Higgs is thus an essential feature of the standard model. The Higgs also develops a mass through a "bare" mass term and interactions with other particles, but due to is scalar nature, the mass it acquires through interactions are as large as the largest mass scale in the theory. Thus, in any unified model, the Higgs mass tends to be enormous. Such a large Higgs mass cannot be, however, since it would ruin the successful perturbation expansion used in all standard model calculations. Thus in order to get the required low Higgs mass, the bare mass must be fine-tuned to dozens of significant places in order to precisely cancel the very large interaction terms. At each order of the perturbation expansion (loop-expansion), the procedure must be repeated. However, if supersymmetric partners are included, this fine-tuning is not needed. The contribution of each supersymmetric partner cancels off the contribution of each ordinary particle. This works only if the supersymmetric partners have masses below the TeV range. Thus, stabilization of the gauge hierarchy is accomplished automatically, as long as supersymmetric particles exist and have masses in the range 100 -1000 GeV. The enormous effort going into searches for supersymmetric particles at CERN, Fermilab, etc. is largely motivated by this argument.

Even though no supersymmetric particles have been discovered, they have all been given names. They are named after their partners. Bosonic ordinary particles have fermonic superpartners with the same name except with the suffix "ino" added, while fermonic ordinary particles have bosonic (scalar) superpartner names with the prefix "s" added. So for example, the photino, Higgsino, Z-ino, and gluino are the partners of the photon, Higgs, Z-boson, and gluon respectively. And the squark, sneutrino, and selectron are the scalar superpartners of the quark, neutrino, and electron respectively. There are several superpartners which have the same quan-

tum numbers and so can mix together in linear combinations. Since these do not necessarily correspond to any one ordinary particle, they are given different names. For example, the photino, Higgsino, and Z-ino can mix into arbitrary combinations called the neutralinos, and the charged W-ino and charged Higgsino combine into particles called charginos.

Finally, an interesting feature of most supersymmetric models is the existence of a multiplicatively conserved quantum number called R-parity, in which each superpartner is assigned $R = -1$, and each ordinary particle is assigned $R = +1$. This quantum number implies that supersymmetric particles must be created or destroyed in pairs, and that the lightest supersymmetric particle (LSP) is absolutely stable; just as the electron is stable since electric charge is conserved and there is no lighter charged particle into which it could decay. This fact is what makes supersymmetric particles dark matter candidates. If supersymmetry exists and R-parity is conserved, then some LSP's must exist from the Early Universe. The only question is how many.

6.2 Relic Abundance in More Detail

The number density of any particle which was once in thermal equilibrium in the Early Universe can be found by solving the relevant set of Boltzmann equations. In most cases only one is needed

$$\frac{dn_\chi}{dt} = -3Hn_\chi - n_\chi^2\langle\sigma v\rangle(\chi\chi \rightarrow \text{ordinary stuff}) + n_{ord}^2\langle\sigma v\rangle(\text{ordinary stuff} \rightarrow \chi\chi),$$

where H is the Hubble constant, n is the number density, t is time, and $\langle\sigma v\rangle$ is the thermally averaged cross section times the relative velocity of the interacting particles. We are using χ to denote the LSP. The first term on the right-hand side is the reduction in number LSP density due to the Hubble expansion, the second term is reduction due to self-annihilation, and the third term is the increase due to particle production. The third term can be simplified using the fact that "ordinary" particles such as quarks and electrons stay in thermal equilibrium throughout period during which the Wimp number density "freezes out" (see Section 4). When thermal equilibrium obtains, creation equals annihilation, so the second and third terms are equal. Therefore one can eliminate the "ordinary particle" cross sections and number densities and find the usual equation

$$\frac{dn}{dt} = -3Hn_\chi - (n_\chi^2 - n_\chi^{eq2})\langle\sigma v\rangle_{annihilation}.$$

Starting at an early time when all particles were in equilibrium, one integrates this equation either numerically or using the standard "freeze-out" approximation [21]. and obtains the number density at $t = 0$ (today). The relic abundance is simply $\Omega_\chi = m_\chi n_\chi/\rho_{crit}$, where m_χ is the mass of the LSP.

The difficult step in obtaining the current day density, is usually the calculation of the annihilation cross section of two LSPs into all standard model particles. In order to perform this calculation, one must first determine which particle is the LSP, and then evaluate all the relevant Feynman diagrams. Going through the list of supersymmetric particles, one finds, basically by process of elimination, that only the sneutrino and neutralino are likely candidates. In the vast majority of models, the neutralino is favored over the sneutrino, so most work has concentrated on the neutralino as dark matter candidate.

For the neutralino, several dozen Feynman diagrams contribute to self-annihilation, including possible annihilation into quarks, leptons, W, Z, and Higgs bosons, and involving most of the super-partners as exchange particles. So in order to perform the calculation one needs to first obtain the mass and couplings of all the supersymmetric particles. Since supersymmetry is broken, the mass terms are unknown, giving rise to many free parameters in the most general supersymmetric model. Usually, in order to simplify things, one considers the "minimal" supersymmetric model, the model with the fewest number of new particles, but still there are many undetermined parameters. So to further simplify, several other assumptions are usually made. In minimal supergravity, some GUT scale assumptions can reduce the number of parameters to just a few. In what follows, we use some, but not all, of the super-gravity assumptions, and have as a result 5 free parameters [22]. The parameters are the gaugino mass parameters M_1 and M_2, the Higgsino mass parameter μ, the pseudoscalar Higgs mass m_A, and the ratio of Higgs vacuum expectation values $\tan\beta$. For any set of parameters, one can calculate all the masses, mixings, and couplings, and then the annihilation cross section. Thus after a long calculation, one finally obtains Ωh^2 in terms of the five parameters. If one obtains a relic abundance in the range $0.025 < \Omega h^2 < 1.0$, then that set of parameters defines a potential dark matter candidate. However, before deciding that this is a dark matter candidate one must ensure that one of the many accelerator experiments that have searched for supersymmetric particles has not already ruled out that model.

6.3 Accelerator Constraints

Extensive unsuccessful searches for the particles involved in supersymmetric models have been performed at particle accelerators throughout the world. This does not yet mean that low-energy supersymmetry is unlikely to exist since only a small portion of the mass range under 1 TeV has been explored. However, substantial regions of prime neutralino dark matter parameter space have been eliminated, and it is important to check this when considering the detectability of any neutralino candidate. One does not want to build a detector only capable of seeing particles ruled out by current experiments. In the following, we demonstrate a method of exploring supersymmetric parameter space taking into account accelera-

tor constraints in a rough way [22]. Note that the same supersymmetric parameters which determine the relic abundance cross sections determine all the particle production and rare decay cross sections. Thus once these parameters are specified, one can compare the model predictions with experimental results. A partial list of relevant experimental results follows. Higgs searches at LEP rule out the lightest scalar Higgs masses below about 45 GeV, and pseudoscalar Higgs masses below about 39 GeV, using cross sections such as $Z \to h\mu^+\mu-$, and $Z \to hA$. LEP chargino searches at the Z pole rule out $m_\chi^\pm$ below 45 GeV, and direct neutralino searches constrain the branching ratio of Z into neutralinos to be less than about 10^{-5}. The squark and gluino searches by CDF give complicated results, but one is probably safe if one limits consideration to squarks with mass larger than 150 GeV. Finally, the recent CLEO measurement of $10^{-4} < \mathrm{BR}(b \to s\gamma) < 4.2 \times 10^{-4}$ has important consequences for neutralinos. This is the decay of bottom quarks into strange quarks plus a photon, and the measurement is within the prediction of the standard model. The impact on supersymmetry comes because this process can also occur via exchange of supersymmetric particles and in many cases these contributions can destroy the experimental agreement with the standard model. So this branching ratio should also be computed for every set of supersymmetric parameters, and models which do not agree with the above constraint should be eliminated. We illustrate the process by considering the grid of models in Figure 1. Since the actual parameter space is five-dimensional, this is just a two- dimensional projection of the parameters. Figure 1(a) shows the entire grid of models, while Figure 1(b) shows the models which are left after eliminating those which violate an accelerator constraint (or other consistency test).

Using just the allowed models we can not plot the neutralino mass vs the relic abundance. The resulting plot (Figure 2) is quite remarkable and can be taken as a hint that supersymmetry may well have something to do with the dark matter problem. Many models fall in the $0.025 < \Omega h^2 < 1.0$ range. Recall that models with $\Omega h^2 > 1$ imply a dark matter density inconsistent with cosmological measurements. Thus dark matter considerations can be used to help the particle physicists in their search for supersymmetry; there is probably little use in considering models which are inconsistent with cosmology (though as experimentalists, it is probably wise that not too much weight is given to such results). On the other hand, models with $\Omega h^2 < 0.025$ are perfectly viable from a particle physics point of view, but predict too little relic abundance to make up all of the dark matter. It is interesting to note, however, that even a relic abundance of $\Omega = 10^{-5}$ would make neutralinos as large a contributor as the microwave background. There was no fine tuning invoked to produce the numerous models with relic abundance in the proper range to be the dark matter, and it seems that no matter what, if stable neutralinos exist, they must be an important contributor to the mass inventory of the Universe.

6.4 Detection techniques

There are several ways of attempting to test the hypothesis that stable neutralinos exist and contribute to the dark matter. History has shown that the most powerful method of discovering new particles is with particle accelerators, so if I had to guess, I would guess that discovery of supersymmetric dark matter will come from CERN. The new LEP 200 machine should be coming on line in a few years, and it has the ability to explore much of the minimal supersymmetric parameter space. The most powerful search will be their Higgs search, and if they find a Higgs which is not the standard model Higgs, I would take it as strong evidence for supersymmetry. New searches for neutralinos and other supersymmetric partners will also be made, so anyone interested in the identity of the dark matter should watch for these results. After LEP 200, the cancelled SSC, had the best chance of discovering supersymmetry, so that cancellation was a big disappointment. Luckily, Europe has picked up the ball and the LHC at CERN has now been funded to search for the Higgs and supersymmetry. Keep in mind that if neutralinos are discovered, and their mass and couplings measured, one could predict the relic abundance using the methods discussed above, and know what contribution they make to the dark matter.

While the accelerators have perhaps the best chance of discovering supersymmetric dark matter, it would be much more satisfying to actually detect the particles in our halo as they move past and through the Earth. This would also allow measurement of the local density of dark matter and establish beyond doubt that the dark matter is non-baryonic cold dark matter. Currently there are two main methods being aggressively pursued.

6.5 Direct Detection

The most exciting result would be direct detection of the Wimp particles. Since we roughly know the speed (~ 270 km/s) and the density ($\rho \sim 0.3$ GeV cm^{-3}), we can say that for a Wimp of mass of order 10-100 GeV, roughly 100,000 dark matter particles a second pass through every square centimeter of the Earth, including our bodies. If they exist, these are very weakly interacting particles, so it is quite rare that one of them will interact at all. In addition, if one does elastically scatter off a nucleus, the deposited energy is usually in the keV to 100 keV range, so extremely sensitive devices must be used. These difficulties, however, have not stopped many groups throughout the world from developing devices capable of detecting Wimps. See references [22,23] for details.

In deciding the size, sensitivity, and energy threshold of a detector, the experimentalist would like to know what event rate one expects in the case that the dark halo consists entirely of Wimps. For a unspecified Wimp, only rough estimates can be made using general arguments [24], but for neutralino Wimps, the elastic scattering cross section and the event rate per kilogram detector per year can be calculated, once the supersymmetric model parameters are chosen. Figure 3 shows

a scatter plot of the rate in a germanium 73 detector, for all the models that pass the accelerator constraints and have relic abundances in the range $0.025 < \Omega h^2 < 1$. The "stripes" in the plot are due to the finite grid we sampled in parameter space, and so the spaces between the stripes should be mentally filled in. A kilogram of germanium was chosen since this is roughly the material and size of one of the most advanced experimental efforts (see below). We see that if neutralinos of around 50 GeV mass make up the dark matter, the expected event rate is probably between 10^{-4} and 1 event/kg/year.

When a Wimp scatters off a nucleus, the nucleus recoils, causing dislocation in the crystal structure, vibrations of the crystal lattice (i.e. phonons or heat), and also ionization. The main difficulties in these experiments come from the fact that the events are rare and that there are many backgrounds which deposit similar amounts of energy on much more frequent time-scales. So in the past few years the main experimental efforts have gone toward increasing the mass of the detectors and discriminating the nuclear recoil signal from the background. Generally the detectors must be operated deep underground at milli-Kelvin temperatures, and be heavily shielded. A illustration of the problem is shown in Figure 4, which shows the background in a germanium detector built by the Berkeley, LBL, UCSB group and operated under the Oroville dam [26,27]. One sees many background processes including lines from radioactive elements and tritium, electron noise at low energy deposited, and a roughly constant background at about one event/kg/day/keV. Comparing this to a typical expected signal in Figure 5, one sees the problem. However, the vast majority of the background comes from gamma rays, while the Wimp signal would be nuclear recoils, and it has been established that gamma rays deposit a much larger fraction of their energy in ionization than in phonons or heat. So the experimentalists measure simultaneously the energy deposited in heat and the energy deposited in ionization and are therefore able to reject perhaps 99% of the background gamma rays [25]. This kind of discrimination is possible only in materials such as germanium and silicon which can be used as ionization detectors, but for other materials such as NaI, and Xenon other effects such as pulse shape or scintillation light may be used to separate the gamma-rays from the nuclear recoils [28]. Using the CDMS (Berkeley/LBL/UCSB/Stanford/Baksan) collaboration as an example [25], the sensitivity of experiments starting to run this year is in the 0.1 to 1 event/kg/year range, and upgraded versions hope to reach 0.01 event/kg/year within a few years. Returning to Figure 3, one sees that there are viable supersymmetric models which will be explored and that a discovery is possible. However, one also sees that a definitive experiment will not be possible within the next few years, since rates below the expected experimental sensitivity are common. However, it is remarkable to realize that these small underground experiments are competing directly with CERN in the race to discover supersymmetry. And the enormous increases in sensitivity these experiments have accomplished in the past few years, leads one to expect further such advances in the future.

6.6 Indirect Detection

A great deal of theoretical and experimental effort has gone into another potential technique for Wimp detection. The idea is that if the halo is made of Wimps, then these Wimps will have been passing through the Earth and Sun for several billion years. Since Wimps will occasionally elastically scatter off nuclei in the Sun and Earth, they will occasionally lose enough energy, or change their direction of motion enough, to become gravitationally captured by the Sun or Earth. The orbits of such captured Wimps will repeatedly intersect the Sun (or Earth) resulting in the eventual settling of the Wimps into the core. As the number density increases over time, the self-annihilation rate $\chi\chi \rightarrow \nu\bar{\nu}$ will increase, resulting in a stream of neutrinos produced in the core of the Sun or Earth. Neutrinos easily escape the Solar core and detectors on Earth capable of detecting neutrinos coming from Sun or Earth have operated for some time. The energy of such neutrinos is roughly 1/2 to 1/3 the mass of the Wimp, so these neutrinos are much higher energy than the MeV scale Solar neutrinos from nuclear reactions that have already been detected. The higher energy of these Wimp annihilation neutrinos make them easier to detect than ordinary solar neutrinos and somewhat compensates for their much fewer numbers. It also makes them impossible to confuse with ordinary solar neutrinos. Thus the presence of a source of high energy neutrinos emanating from the centers of the Sun and Earth would be taken as evidence for Wimp dark matter. While the above chain of reasoning may seem long, I don't know of any holes in it, and several experimental groups are in the process of designing and building detectors capable of seeing such a neutrino signal. For example, the IMB and Kamionkande proton decay detectors have already been used to set (very weak) limits on Wimp dark matter using this technique [29]. The MACRO monopole search detector has also looked for this signal [29]. Several new detectors are being created which should be substantially more sensitive. For this signal, it is not the mass of the detector which is relevant, but the surface area. Neutrinos from the core of the Sun or Earth produce muons in the atmosphere and rock around the detectors, and it is primarily these muons the detectors watch for. Muons are also copiously created by cosmic rays entering the Earth's atmosphere, so there is a substantial background of "downward" traveling muons. These detectors, then are located deep underground, where the rock shields many of the background muons, and they also focus on "upward" traveling muons, which are much more likely to have been created by neutrinos that have traveled through Earth and interacted in the rock just below the detector. Thus surprisingly, the best way to see high energy neutrinos from the Sun is to go deep underground at night (when the Sun is "under" the Earth)! Since the range of the muons depends mostly on the energy of the neutrinos, The number of muons detected depends mostly on the surface area of the detector. So the new generation of detectors are designed to have very large surface areas. Examples include MACRO, superkamiokande, AMANDA, DUMAND, and NESTOR [30].

As an example, consider the AMANDA detector [30] which is being prototyped in Antarctica. There are several ways to detect high energy muons, one of which is to measure the Cerenkov light emitted as they travel faster than light-speed in some medium. AMANDA places strings of phototubes deep in the Antarctic ice, in order to detect the Cerenkov light thus emitted. So far four long strings have been deployed at depths in the kilometer range. These deep holes are dug in a day using just hot water! The Antarctic ice is extremely clear and light can travel large distances. Small lasers were also put down in order to measure the ice transparency and test the feasibility of the idea. The initial results were both bad and good. The collaboration found bubbles in the ice substantially larger than the "ice experts" had indicated. These meant that the Cerenkov light diffused too much to be useful in detecting muons. However, the size of the bubbles is decreasing with depth, and they expect by placing their next phototube strings deeper the bubble problem will disappear. The good news was that the ice was substantially more transparent that they had expected, meaning that they can place their next strings further apart, thereby increasing the effective surface area of their detector.

How will detectors such as AMANDA fare in the detection of Wimps? Using the cross sections, etc. calculated from the supersymmetric models one can calculate the density of neutralinos in the Sun and Earth, and then the annihilation rate, and then the number of neutrinos incident on Earth, and then the number of muons produced, and finally the number of muons detected. An example of such a calculation is shown in Figure 6, for precisely the same models shown in Figure 3. The AMANDA detector may have an effective area of 1000 m^2, so as you can see the story is somewhat the same as for direct detection. There is a region of supersymmetric parameter space which will be probed by these indirect detectors, but there are many possible sets of model parameters for which indirect detection is not possible without much more sensitive detectors. A comparison of direct and indirect detection methods leaves one with the impression that for a typical neutralino a kilogram of direct detector germanium has about the same sensitivity as $10^4 - 10^6$ m^2 of indirect detector [31].

7. Baryonic Dark Matter (Machos)

Probably the most exciting development in the dark matter story is the detection of Machos by three separate groups [32,33,34] All three groups monitored millions of stars [35], either in the LMC or in the galactic bulge, for signs of gravitational microlensing, and all three groups have found it. It has now become clear that these objects constitute some new component of the Milky Way, but they do not constitute the bulk of the dark matter. Thus, the Macho search results gives strong impetus to the search for particle dark matter. However, the more than 60 detected microlensing events are far in excess of predictions of standard Galactic models and imply that the Galaxy is probably quite different than was thought previously.

7.1 Microlensing

Microlensing has arrived as a powerful new tool for exploring the structure of our Galaxy. However, from the dark matter point of view, I'd like to note that the current experiments may have the capability to give a definitive answer to the question of whether the dark matter in our Galaxy is baryonic. The microlensing searches are probably sensitive to any objects in the range $\sim 10^{-8} M_\odot < m < 10^3 M_\odot$, just the range in which such objects are theoretically allowed to exist. Objects made purely of H and He with masses less than $\sim 10^{-9} - 10^{-7} M_\odot$ are expected to evaporate due to the microwave background in less than a Hubble time, while objects with masses greater than $\sim 10^3 M_\odot$ would have disrupted known globular clusters.

The idea of microlensing rests upon Einstein's observation that if a massive object lies directly on the line-of-sight to a much more distance star, the light from the star will be lensed and form a ring around the lens. This "Einstein ring" sets the scale for all the microlensing searches, and in the lens plane, the radius of that ring is given by

$$r_E = 610 R_\odot [\frac{m}{M_\odot} \frac{L}{\mathrm{kpc}} x(1-x)]^{1/2},$$

where $R_\odot$ and $M_\odot$ are the solar radius and mass, m is the Macho mass, L is the distance to the star being monitored, and x is the distance to the Macho divided by L.

In fact, it is extremely unlikely for a Macho to pass precisely on the line-of-sight, but if there is a near miss, two images of the star appear separated by a small angle. For masses in the stellar range and distances of galactic scale this angle is too small to be resolved, but the light from both images add and the star appears to brighten. The amount of brightening can be large, since it is roughly inversely proportional to the minimum impact parameter b/r_E. Since the Macho, Earth, and source star are all in relative motion, the star appears to brighten, reaches a peak brightness, and then fades back to its usual magnitude. The brightening as a function of time is called the "lightcurve" and is given by

$$A(u) = \frac{u^2+2}{u\sqrt{u^2+4}}, \qquad u(t) = [u_{min}^2 + (2(t-t_0)/\widehat{t})^2]^{1/2},$$

where A is the magnification, $u = b/r_E$ is dimensionless impact parameter, t_0 is the time of peak amplification, $\widehat{t} = 2r_E/v_\perp$ is the duration of the microlensing event, $v_\perp$ is the transverse speed of the Macho relative to the line-of-sight, and u_{min} is value of u when $A = A_{max}$. Thus the signature for a microlensing event is a time-symmetric brightening of a star occurring as a Macho passes close to the line-of-sight. When a

microlensing event is detected, one fits the lightcurve and extracts A_{max}, t_0, and $\widehat{t}$. The primary physical information comes from $\widehat{t}$, which contains the Macho velocity, and through r_E the Macho mass and distance. Unfortunately, one cannot uniquely find all three pieces of information from the measurement of $\widehat{t}$. However, statistically, one can use information about the halo density and velocity distribution, along with the distribution of measured event durations to gain information about the Macho masses. Using a standard model of the dark halo, Machos of jupiter mass ($10^{-3}M_\odot$) typically last 3 days, while brown dwarf mass Machos ($0.1M_\odot$) cause events which last about a month [Paczyński,49].

In order to perform the experiment, a large number of stars must be followed, since, assuming a halo made entirely of Machos, the probability of any Macho crossing in front of a star is about 10^{-6}. Thus many millions of stars must be monitored in order to see a handful of microlensing events. In addition, if one wants to see microlensing from objects in the dark halo, the monitored stars must be far enough away so that there is a lot of halo material between us and the stars. Therefore, the best stars to monitor are those in the Large and Small Magellanic Clouds (LMC and SMC) at distances of 50 kpc, and 60 kpc respectively, and also stars in the galactic bulge, at 8 kpc.

There are several experimental groups that have undertaken the search for microlensing in the LMC and galactic bulge and have returned results. The EROS collaboration, has reported 3 events towards the LMC [33], the OGLE group has reported about 15 events towards the bulge [34], and the DUO collaboration has about a dozen preliminary events towards the bulge [36]. Our collaboration has seen about 5 events towards the LMC [32,37,38], and about 60 events towards the bulge [39,40,41]. We are also monitoring the SMC, but have yet to analyze that data. In what follows I will concentrate on MACHO collaboration data.

7.2 The MACHO Collaboration Experiment

The MACHO experiment is led by Charles Alcock and is a collaboration of Physicists and Astronomers from Lawrence Livermore National Lab, The UC Berkeley Center for Particle Astrophysics, Mount Stromlo and Siding Spring Observatory, The University of Washington, Oxford, McMaster, and UC San Diego. We have essentially full-time use of the 1.27-meter telescope at Mount Stromlo Observatory, Australia, for a period of about 8 years from July 1992. In order to maximize throughput a dichroic beamsplitter and filters provide simultaneous images in two passbands, a 'red' band (approx. 5900–7800 Å) and a 'blue' band (approx. 4500–5900 Å). Two very large CCD cameras [42] are employed at the two foci; each contains a 2×2 mosaic of 2048×2048 pixel Loral CCD imagers, giving us a sky coverage of 0.5 square degrees. Observations are obtained during all clear nights and part nights, except for occasional gaps for telescope maintenance. The default

exposure times are 300 seconds for LMC images, 600 sec for the SMC and 150 seconds for the bulge, so over 70 exposures are taken per clear night.

Photometric measurements from these images are made with a special-purpose code known as SoDoPHOT [43], derived from DoPHOT [44]. For each star, the estimated magnitude and error are determined, along with 6 other parameters (quality flags) measuring, for example, the crowding, and the χ^2 of the point-spread-function fit. It takes about an hour on a Sparc-10 to process a field with 500,000 stars, and so with the computer equipment available to us we manage to keep up. The set of photometric data points for each field are re-arranged into a time-series for each star, combined with other relevant information including the seeing and sky brightness, and then passed to an automated analysis to search for variable stars and microlensing candidates [45]. The total amount of data collected to date is more than two Terabytes, but the time-series database used for analysis is only about 100 Gbytes.

7.3 Event Selection

Most of the stars we monitor are constant within our photometric errors, but about one half of one percent are variable. The MACHO database, as repository for the largest survey ever undertaken in the time domain, is an extremely valuable resource for studies of variable stars. From our first year LMC data alone we have already identified about 1500 Cepheid variables, 8000 RR Lyrae, 2200 eclipsing binaries, and 19000 long period variables. Example lightcurves from each of these classes can be found in reference [46,47]. We also have many rare variables, and have given the first conclusive evidence of 1st overtone pulsation in classical Cepheid's [48]. We have also observed what may turn out to be entirely new types of variable stars [46].

Given that the incidence of stellar variability, systematic error, and other sources of stellar brightening is much higher than the incidence of microlensing, how can one hope to discriminate the signal from the background among the tens of millions of stars we monitor nightly? Fortunately, there are several very powerful microlensing signatures which exist:

1. High amplification. Very high amplifications are possible, so we can set our A_{max} threshold high enough to avoid many types of systematic error background.

2.) Unique shape of lightcurve. Only 5 parameters are needed to completely specify the 2-color lightcurve.

3.) Achromaticity. Lensing magnification should be equal at all wavelengths, unlike brightenings caused by most types of stellar variability.

4.) Microlensing is rare. The chance of two microlensing events occurring on the same star is so small, that any star with more than one "event" can be rejected as a microlensing candidate.

5.) Statistical tests: The distribution of peak magnifications A_{max} is known a priori. Microlensing should occur with equal likelihood on every type and luminosity of star, unlike known types of stellar variability. New microlensing events should be discovered each year at a constant rate.

6.) Alert possibility. Our alert system is now working and we can catch microlensing before the peak and get many measurements of high accuracy. Other spectral and achromaticity tests can also be performed in follow-up mode.

Using these criteria, as well as others, we have found it possible to pick out microlensing candidates from variable stars, etc. For example, starting with about 9.5 million lightcurves from our first year LMC database, we remove all but 3. These are shown in Figure 7.

One of these events is clearly superior in signal/noise to the others, and we have confidence in the microlensing label. It has $A_{max} = 7.2$, and $\widehat{t} = 35$ days. The other two, while passing all our cuts, and certainly consistent with microlensing, are less certain to be actual microlensing. We should note that our alert system has found a couple more high signal/noise LMC microlensing events, which are not included here, since we have performed efficiency calculations only on the first year data set.

Now, if we had found only these 3 events towards the LMC, we would not be as confident as we are, that we have seen microlensing. However, we have many more events towards the galactic bulge, and some of these are of incredibly high signal/noise. We cannot use the same selection criteria for the bulge as for the LMC since our observing schedule towards the bulge is different, and the bulge stellar population, distance, crowding, and extinction are different, but using the same statistics, we can make a similar selection procedure. We find about 43 candidates in our first year data (and since then a few dozen more in our alert system). Examples of lightcurves from the bulge are shown in Figure 8. Some of these events are truly beautiful, with durations of many months and magnifications of almost 20. Coupled with the dozen events from the OGLE collaboration, I think little doubt remains that microlensing has been seen.

7.4 Detection Efficiency

What do the microlensing events mean for the dark matter question? In order to answer, we need to know the efficiency with which our system can detect microlensing. This is a non-trivial calculation. In order to calculate our efficiencies, we add simulated stars to real images, and then artificially brighten them. We run the photometry code on these simulated images and find what the photometry

code returns when a star brightens under different atmospheric and crowding conditions. These results are incorporated into a large Monte Carlo in which simulated microlensing events are added to our actual (non-microlensing) data and fed into the same time-series analysis and selection procedure which produced the 3 LMC microlensing candidates. Thus we have explicitly taken into account inefficiencies caused by bad weather and system down time, our analysis and selection procedure, as well as blending of the underlying stars due to crowding, and systematic errors in our photometry. Since in order to calculate the expected number of events, we need to integrate a theoretical microlensing rate over our measured efficiency, we need efficiency ϵ, as a function of $\widehat{t}$. The function ϵ can be found in reference [37,38]. Once ϵ is calculated, the number of expected events is $N_{exp} = E \int \frac{d\Gamma}{d\widehat{t}} \epsilon(\widehat{t}) d\widehat{t}$, where our total exposure $E_{LMC} = 9.7 \times 10^6$ star-years, and $d\Gamma/d\widehat{t}$ is a differential microlensing rate which can be calculated given a model of the dark halo [49,50].

7.5 Interpretation of LMC Events

Using our sample of microlensing events, there are two complementary analyses which can be performed. First, we can set a conservative limit on the Macho contribution to the dark halo. Since we know our efficiencies, and we have certainly not seen more than 3 microlensing events from halo objects, any halo model which predicts more than 7.75 events can be ruled out at the 95% C.L. This result will be independent of whether or not all three candidate events are due to microlensing, and independent of whether or not the lenses are in the dark halo. Second, if we make the further assumption that all three events are due to microlensing of halo objects, we can estimate the mass of the Machos and their contribution to the mass of the dark halo.

In order to do either analysis we need a model of the dark halo. We need to know the total mass of the halo, and we need the density and velocity distribution to calculate an expected microlensing rate. The main constraints on the halo come from the Milky Way rotation curve, which is not as well determined as rotation curves in other galaxies. Constraints from the orbits of satellite galaxies also exist, but there is considerable uncertainty in both the total halo mass and the expected microlensing rate coming from uncertainty in the size and shape of the Milky Way halo [51,52,50]. Using a very simple, but commonly used halo model [49], we can calculate the number of expected events as described above, and the results are shown in Figure 9. If the Milky Way has a standard halo consisting entirely of Machos of mass $0.001 M_\odot$ then we should have seen more than 20 events, with fewer events at larger or smaller masses. However, even if the halo dark matter consists of Machos, it is very unlikely that they all have the same mass. Fortunately, it can be shown [49], that if one rules out all halos made of unique Macho mass between masses m_1 and m_2, then one has ruled out a halo consisting of ANY distribution of masses as long as only masses between m_1 and m_2 are included. Thus we can make

the powerful conclusion that a standard halo consisting of any objects with masses between $8 \times 10^{-5} M_\odot$ and $0.3 M_\odot$ has been ruled out by our first year LMC data.

As mentioned above, there is no strong reason to believe that the Milky Way halo is precisely as specified in the standard halo, and we would like to test the robustness of the important results above by considering a wider range of viable halo models. To this end, we have investigated a class of halo models due to Evans [53]. These models have velocity distributions which are consistent with their density profiles, and allow for halos which are non-spherical, and which have rotation curves which gently rise or fall. A description of the parameters that specify these models, along with microlensing formulas can be found in Alcock, *et al.* [50]. Basically we consider models which give rotation velocities within 15% of the IAU standard value of 220 km/sec, at the solar circle (8.5 kpc) and twice the solar circle. As pointed out by Evans and Jijina [54], the contribution of the stellar disk plays an important role in the predicted microlensing rate. This is because much (or even most) of the rotation speed could be due to material in the disk, so we consider various size disks, as well.

Using these models, we find strong limits are found on heavy halo models, while only very weak limits are found on light halo models. This is because microlensing is sensitive not to the total mass in the halo, but only to the mass in Machos. So one can get a much more model independent limit on the Macho content of the halo by limiting the *total mass in Machos*, rather than the *Macho fraction* of the halo. A more robust statement of our first year LMC microlensing results is thus that objects in the $2 \times 10^{-4} - 2 \times 10^2 M_\odot$ range can contribute no more than $3 \times 10^{11} M_\odot$ to the dark halo, where we consider the halo to extend out to 50 kpc. The standard halo has $4.1 \times 10^{11} M_\odot$ out to this radius, and so is ruled out as before, but much smaller, all Macho halos, would be allowed. It should be clear that in order to get good information on the Macho fraction of the halo, more work is needed on the total mass of the halo. This requires better measurement of the Milky Way parameters and rotation curve. Microlensing measurements themselves may also be able to help [52,51,50].

The limits above are valid whether or not the three events shown in Figure 7 are due to microlensing of halo objects. However, if we make the additional assumption that they are, we can go beyond limits and estimate the Macho contribution to the halo, and also the masses of the Machos. The results obtained, especially on the lens masses, depend strongly on the halo model used, so keep in mind that it is not clear that all three events are microlensing, and it is certainly not known that they are due to objects residing in the galactic halo. Proceeding anyway, we can construct a likelihood function as the product of the Poisson probability of finding 3 events when expecting N_{exp} and the probabilities of drawing the observed $\widehat{t}$'s from the calculated model duration distribution [50,37,38]. The resulting likelihood contours can be found in references [37] and [38]. We find that for a standard halo, a macho fraction of $\sim 20\%$ is most likely, with Macho masses in the $0.01 - 0.1 M_\odot$

range likely. Note that the errors in these estimates are very large due to the small number statistics, and that there is an enormous additional uncertainty due to the halo model. However, once again, the maximum likelihood estimate of the total mass in Machos is quite model independent and is about $8 \times 10^{10} M_{\odot}$. Since the mass in known stars, gas, etc. is only about $6 \times 10^{10} M_{\odot}$, we see this would be a major new component of the Milky Way if it is confirmed to exist.

7.6 Interpretation of Bulge Events

The large number of events we (and the OGLE group [34]) have found towards the galactic center came as a great surprise to everyone. The line-of-sight toward the bulge goes though the stellar disk, so bulge microlensing is sensitive to halo dark matter, disk stars, and any disk dark matter which might be present. The early predictions [55,56,57] included all these sources, but still predicted many fewer events than have now been observed. It seems the microlensing experiments have discovered a new component of the Milky Way. A standard way of quoting the microlensing probability is the optical depth τ, which is the probability that any given source star is lensed by a magnification of 1.34 or greater. Optical depth has larger statistical errors than the event rate, but has the great advantage of being independent of the masses of the lenses. Early predictions of bulge microlensing were in the 10^{-6} range [55,56,57], while using the sample of events above we find $\tau_{est} = 3.9^{+1.8}_{-1.2} \times 10^{-6}$ [41]. We have not finished the complete efficiency calculation for our bulge events, so this estimate uses a sub-sample of 15 giant star events, for which our preliminary efficiencies should be acceptable [41].

Several models have now been proposed to explain the high microlensing rate. They include [58, 59, 60]

1) A "heavy" disk. Perhaps the disk of the Milky Way is substantially more massive than normally considered.
2) A "bar" at small inclination. Perhaps the Milky way is not a grand design spiral as usually assumed, but is a barred spiral, with a very large bar, previously overlooked since it points nearly toward us.
3) A highly flattened, or disk-like halo.
4) Some combination of the above, and/or extra material in the bulge.

The suggestion of a Galactic bar has been around for a few years, and seems to be corroborated by other data [61], though it is still not clear whether this alone is sufficient to explain the microlensing data. Extensive work is being undertaken in trying to resolve these questions. One method is to map out the bulge area with microlensing. A bar-like structure will give a different pattern of microlensing than a disk-like structure. Use of a satellite, or the fine-structure of the microlensing lightcurve has also been suggested [62,63].

7.7 Advantages of Having Many Events

There are two main advantages of having several times more events than we originally thought we would have. First, we can do statistical tests on the data. For example, simple geometry predicts a specific distribution of maximum amplifications. Basically, every lens/line-of-sight impact parameter should be equally likely, so the distribution of u_{min}'s should be uniform (taking into account that our efficiency for detecting high magnification (low u_{min}) events is larger). We have performed a Kolmogorov-Smirnov (K-S) test on the bulge events and find good consistency with the microlensing hypothesis. Thus the microlensing interpretation of these events is greatly strengthened.

The second advantage of having many events, is that rare events can be found. For example events of high magnification or long duration should occur occasionally. For some types of rare events additional important information concerning the Macho mass/velocity/distance can be extracted. For example, in reference [64] we show an event which lasted about 1/2 year, during which time the Earth had a chance to travel part way around the Sun. This gave our telescope two different perspectives on the lens, resulting in a parallax event. Thus the lightcurve does not fit the naive amplification formula presented earlier. Including the Earth's motion, we find a good fit, and discover that the Macho was moving with a projected transverse velocity of 76 ± 6 km/sec. The Macho mass is determined by a combination of this velocity, the event duration, and the distance to the Macho, so for such parallax events there is a one-to-one relationship between the Macho mass and distance. In this case the Macho could be either a brown dwarf star in the galactic bulge, an M-dwarf star at a distance of 2 to 6 kpc, or a more massive star quite nearby.

Another rare type of microlensing event is shown in reference [47,40]. This lightcurve is characteristic of lightcurves formed by binary lenses. This particular event was first seen by the OGLE group [34], and detailed analysis will again give information as to the lens masses, distances and velocities. An exciting aspect of such a binary Macho detection, is the possibility of detecting planets around Machos. Given that some of the lenses we observe are in fact low mass stars, it is possible to observe caustic crossing such as mentioned above, for planets even down to Earth mass [65,66]. Thus microlensing may well be the best way to discover and get statistics on extra-solar planets.

7.8 Macho Conclusion

The microlensing experiments have given robust and strong limits on the baryonic content of the halo. Much more data from the LMC and SMC will be available soon, so we expect the statistics to improve in the near future. The LMC events, if interpreted as due to halo microlensing, allow a measurement of the baryonic contribution to the halo, which is around 20% for a standard halo. In this case, the

most likely Macho contribution to the Milky Way halo mass is about $8 \times 10^{10} M_{\odot}$, which is roughly the same as the disk contribution to the Milky Way mass. However, the whole story has been made more complicated (and exciting) by the much larger than expected number of bulge microlensing events. These events imply a new component of the Galaxy, and until the nature of this new component is known, unambiguous conclusions concerning the LMC events will not be possible. For example, if the Milky Way disk is much larger than usually considered, a much smaller total halo mass will be required, and so even an all Macho halo might be allowed. Alternatively, the new Galactic component which is giving rise to the bulge events, may also be giving rise to the LMC events, and the Macho content of the halo could be zero. Fortunately, much more data is forthcoming, and many new ideas have been proposed. Microlensing is fast becoming a new probe of Galactic structure, and beside the original potential to discover or limit dark matter, may well produce discoveries such as extra-solar planetary systems.

8. Conclusions

The dark matter situation has changed dramatically in the past few years. Not long ago, people agreed that the dark matter existed, but had little hope of knowing what it actually consisted of. Now strong detection efforts are underway for many of the best candidates. For Machos, first results are already in, and it seems quite probable that the bulk of the dark matter does not consist of Machos in the Earth to brown dwarf mass range. There is still a "baryonic dark matter" window for exotic objects in the solar to 1000 solar mass range. Turning to Wimps, we found that these are excellent dark matter candidates for a variety of reasons, and that three methods of detection are being vigorously pursued: high energy accelerators, direct detection, and via high energy neutrinos from the Sun. Axions also are fine dark matter candidates, and the new microwave cavity experiments will for the first time probe some of the best axion parameter space. However, no experiments capable of definitively ruling out either axion or Wimp candidates are underway, so there is the chance that either could be the dark matter without us discovering it.

No one has yet found a method to directly detect a light neutrino component of the dark matter, though interest in these as candidates for the "hot dark matter" component in a mixed hot plus cold dark matter galaxy formation scenario is very high. For neutrinos, the most promising method is to measure the masses via neutrino oscillation experiments, and then calculate the relic density using the big bang theory. Indirect and preliminary evidence for such neutrino oscillations already exists, so experiments capable of actually determining neutrino masses should be watched with great interest by all astrophysicists.

In conclusion, this is a very active field, and remarkably, there is a reasonable chance of discovering the nature of the dark matter within the next few years.

We thank Andrew Gould, George Fuller, Joel Primack, and members of the MACHO collaboration for valuable help. We acknowledge support from a DoE OJI Award, the NSF Center for Particle Astrophysics (AST-8809616), the Alfred P. Sloan foundation, and a Cotrell Scholars Award.

References

1. Ashman, K.M., 1992. PASP, 104, 1109.
2. Binney, J. & Tremaine, S. 1987, Galactic Dynamics (Princeton University Press, Princeton)
3. Blitz, L., Fich, M., and Stark, A. A., ApJ Supp. 49, 183 (1982)
4. Merrifield, M.R. AJ, 103, 1552 (1992).
5. Zaritsky, D. *et al.*, 1989, ApJ, 345, 759.
6. C.S.Kochanek, e-print, astro-ph 9505068 (1995).
7. J.A.Tyson & P.Fischer, ApJ Lett. 446, L55 (1995).
8. U. G. Briel, J. P. Henry, & H. Bohringer, Astr. Astrophys. 259, L31 (1992).
9. White, S.D.M., *et al.* Nature, 366, 429 (1993).
10. Dekel, A, 1994, ARA&A, 32, 371.
11. A. Yahil, T. Walker, and M. Rowan-Robinson, Astrophys. J. Lett. **301**, L1 (1986).
12. M. Davis and A. Nusser, astro-ph/9501025.
13. K. A. Olive, G. Steigman, D. N. Schramm, T. P. Walker, and H. Kang, Astrophys. J. **376**, 51 (1991).
14. M. S. Smith, L. H. Kawano, and R. A. Malaney, Astrophys. J. Suppl. **85**, 219 (1993).
15. T. P. Walker *et al.*, Astrophys. J. **376**, 51 (1991).
16. For example, F.DePaolis, *et al.*, A&A 295, 567 (1995); F.DePaolis, *et al.*, Phys. Rev. Lett. 74, 14 (1995).
17. Begeman, K.G., Broeils, A.H., & Sanders, R.H. 1991. *M.N.R.A.S.* **249,** 532.
18. for example, Turner, M.S. 1990, *Physics Reports* **197,** 67; Raffelt, G.G. 1990, *Physics Reports* **198,** 1.
19. K. Van Bibber, *et al.*, Int. J. Mod. Phys. D3, 33 (1994).
20. C. Hagmann, *et al.*, Phys. Rev. D42, 1297 (1990).
21. Kolb, E.W. & Turner, M.S. 1990. *The Early Universe,* (Addison-Wesley, Redwood City, California).

22. Jungman, G. Kamionkowski, M., & Griest, K., 1995, to appear in Physics Reports.

23. Proceedings of the 5th Workshop on Low Temperature Devices, Berkeley 1993, in J. Low Temp. Phys. 93, 185 (1993); J.R.Primack, B.Sadoulet, & D.Seckel, Ann.Rev.Nucl.Part.Sci., B38, 751 (1988); P.F.Smith & J.D.Lewin, Phys. Rep. 187, 203 (1990).

24. Griest, K. & Sadoulet, B., in *Dark Matter in the Universe*, eds. Galeotti, P., & Schramm, D.N. (Kluwer, Netherlands, 1989).

25. P.D.Barnes *et al.*, J. Low Temp. Phys. 93, 79 (1993); T.Shutt *et al.*, Phys. Rev. Lett. 65, 1305 (1992); *ibid.* 3531 (1992).

26. Data acquired by the UCB/UCSB/LBL experiment at Oroville kindly provided by A. Da Silva, unpublished.

27. D. O. Caldwell *et al.*, Phys. Rev. Lett. **61** (1988) 510.

28. for example, N.Spooner & P.F.Smith, Phys. Lett. B314, 430 (1993); A.Bottino *et al.*, Phys. Lett. B293, 460 (1992); K.Fushimi, *et al.*, Phys. Rev. C47, 425 (1993); G.J.Davies *et al.*, Phys. Lett. B320, 395 (1994).

29. M.Mori *et al.* (Kamionkande), Phys. Rev. D48, 5505 (1993); J.M.LoSecco *et al.* (IMB), Phys. Lett. B188, 388 (1987); E.Diehl, (MACRO) Ph.D thesis, University of Michegan (1994).

30. R.J.Wilkes, in proceedings of 22nd SLAC Summer Institute on Particle Physics, Stanford 1994; D.M.Lowder *et al.*, Nature 353, 331 (1991); L.Resvanis, Europhys. News 23, 172 (1992).

31. M.Kamionkowski, K.Griest, G.Jungman, & B.Sadoulet, Phys. Rev. Lett. 74, 5174 (1995).

32. Alcock, C., *et al.*, 1993, Nature, 365, 621.

33. Aubourg, E., *et al.*, 1993, Nature, 365, 623; Beaulieu J.P., *et al.*, 1994, preprint.

34. Udalski, A., *et al.*, 1993, Acta Astronomica, 43, 289; Udalski, A., *et al.*, 1994, Acta Astronomica, 44, 165; Udalski, A., *et al.*, 1994, Acta Astronomica, 44, 227; Udalski, A., *et al.*, 1994, ApJ Lett., 436, L103.

35. Paczyński, B, 1986, ApJ, 304, 1.

36. C. Alard, private communication.

37. Alcock, *et al.*, 1995, Phys. Rev. Lett. 74, 2867.

38. Alcock, C., *et al.*, 1995, to appear in ApJ.

39. Alcock, C., *et al.*, ApJ 445, 133 (1995).

40. Bennett, D.P. *et al.*, 1994, Proceedings of the 5th Astrophysics Conference in Maryland: Dark Matter.

41. Alcock, C., *et al.*, 1995, in preparation.

42. Stubbs, *et al.*, 1993, SPIE Proceedings, 1900, 192.

43. D.P.Bennett 1995, in preparation.

44. Schechter, P.L., Mateo, M., & Saha, A., 1994, PASP, 105, 1342.

45. Griest, K. *et al.* 1995, in preparation.

46. Cook, K., *et al.*, 1995, Proceedings of IAU Colloquium 155: Astrophysical Applications of Stellar Pulsation, Cape Town, February 1995, ASP Conference Series, ed. R.Stobie.

47. K.Griest *et al.*, proceedings of the Pascos/Hopkins Symposium, Baltimore, Maryland (World Scientific 1995).

48. C.Alcock, 1995 *et al.*, AJ, 109, 1653.

49. Griest, K., 1991, ApJ, 366, 412.

50. Alcock, *et al.*, 1995, ApJ 449, 28.

51. Gates, E.I., Gyuk, G. & Turner, M.S., 1995, Phys. Rev. Lett., 74, 3724.

52. Sackett, P. & Gould, A., 1994. ApJ, 419, 648.

53. Evans, N.W., 1993. MNRAS, 260, 191; Evans, N.W., 1994, MNRAS, 267, 333.

54. Evans, N.W., & Jijina, J., 1994. MNRAS, 267, L21.

55. Griest, K., *et al.*, 1991, ApJ Lett., 372, L79.

56. Paczyński, B. 1991, ApJ Lett., 371, L63.

57. Kiraga M., and Paczyński, B. 1994, ApJ Lett., 430, L101.

58. C.H.Han & A.Gould, ApJ 449, 521 (1995).

59. Zhou, H.S., Spergel, D.N. & Rich, R.M., 1994, ApJ Lett., 440, L13.

60. Paczyński, B., *et al.*, 1994 ApJ Lett., 435, L113.

61. For example see, D.N.Spergel, in "The Center, Bulge, and Disk of the Milky Way", ed. L.Blitz (Kluwer Academic Press, Dordrecht, 1992).

62. A.Gould, ApJ 444, 556 (1995).

63. A.Gould, ApJ Lett. 441, L21 (1995).

64. C.Alcock *et al.*, to appear in ApJ Lett. 1995.

65. Mao, S. & Paczyński, B., 1991, ApJ Lett., 374, L37.

66. Gould, A. & Loeb, A., 1992, ApJ, 396, 101.

Figure Captions

Figure 1. Parameter space in the minimal supersymmetric model. Only two of the five dimensions (μ and M_2) are displayed. Panel (a) shows the starting grid of parameters choices, and panel (b) shows the models left after eliminating models which violate any of several accelerator constraints (from [22]).

Figure 2. Scatter plot of relic neutralino density vs. neutralino mass for the set of supersymmetric models discussed in the text. Laboratory constraints from LEP measurements and Br($b \to s\gamma$) are enforced. Models between the lines drawn at $\Omega_\chi h^2 = 0.025$ and $\Omega_\chi h^2 = 1$ are compatible with neutralino dark matter (from [22]).

Figure 3. Predicted rate in a ^{73}Ge cryogenic detector vs neutralino mass for the allowed dark-matter models above (from [22]).

Figure 4. Measured gamma-ray background in an underground high-purity germanium ionization detector (data acquired by the UCB/UCSB/LBL experiment at Oroville [26,27]. Various gamma-ray lines are identified, as is the end point of the broad tritium spectrum. The rapid rise at low Q is the electronic noise (from [22]).

Figure 5. Theoretical differential event rate for WIMPS of various masses hitting a germanium target. WIMP masses are labeled in GeV. An arbitrary cross section of $\sigma_0 = 4 \times 10^{-36}\mathrm{cm}^2$ was chosen with standard values for the other parameters. Note the rate axis scale is 100 times *smaller* than in Fig. 4, and the cross section chosen is very high for neutralinos (from [22]).

Figure 6. Indirect-detection rate vs neutralino mass. The sum of the rates for upward muons from both the Sun and Earth is shown. Currently planned experiments will be sensitive in the $10^{-2}\mathrm{m}^{-2}\mathrm{yr}^{-1}$ to $10^{-4}\mathrm{m}^{-2}\mathrm{yr}^{-1}$ range (from [22]).

Figure 7. The three observed stellar lightcurves that we interpret as gravitational microlensing events are each shown in relative flux units (red and blue) vs time in days. The solid lines are fits to the theoretical microlensing shape (from [37]).

Figure 8. Example lightcurves from first year bulge data. Four of the 43 microlensing events are shown (from [46,47]).

Figure 9. The lower panel shows the number of expected events predicted from the standard model halo with a delta function mass distribution. Given three observed events, points above the line drawn at $N_{exp} = 7.7$ are excluded at the 95% CL. The upper panel shows the 95% CL limit on the halo mass in MACHOs within 50 kpc of the galactic center for the model. Points above the curve are excluded at 95% CL while the line at $4.1 \times 10^{11} M_\odot$ shows the total mass in this model within 50 kpc (from [37]).

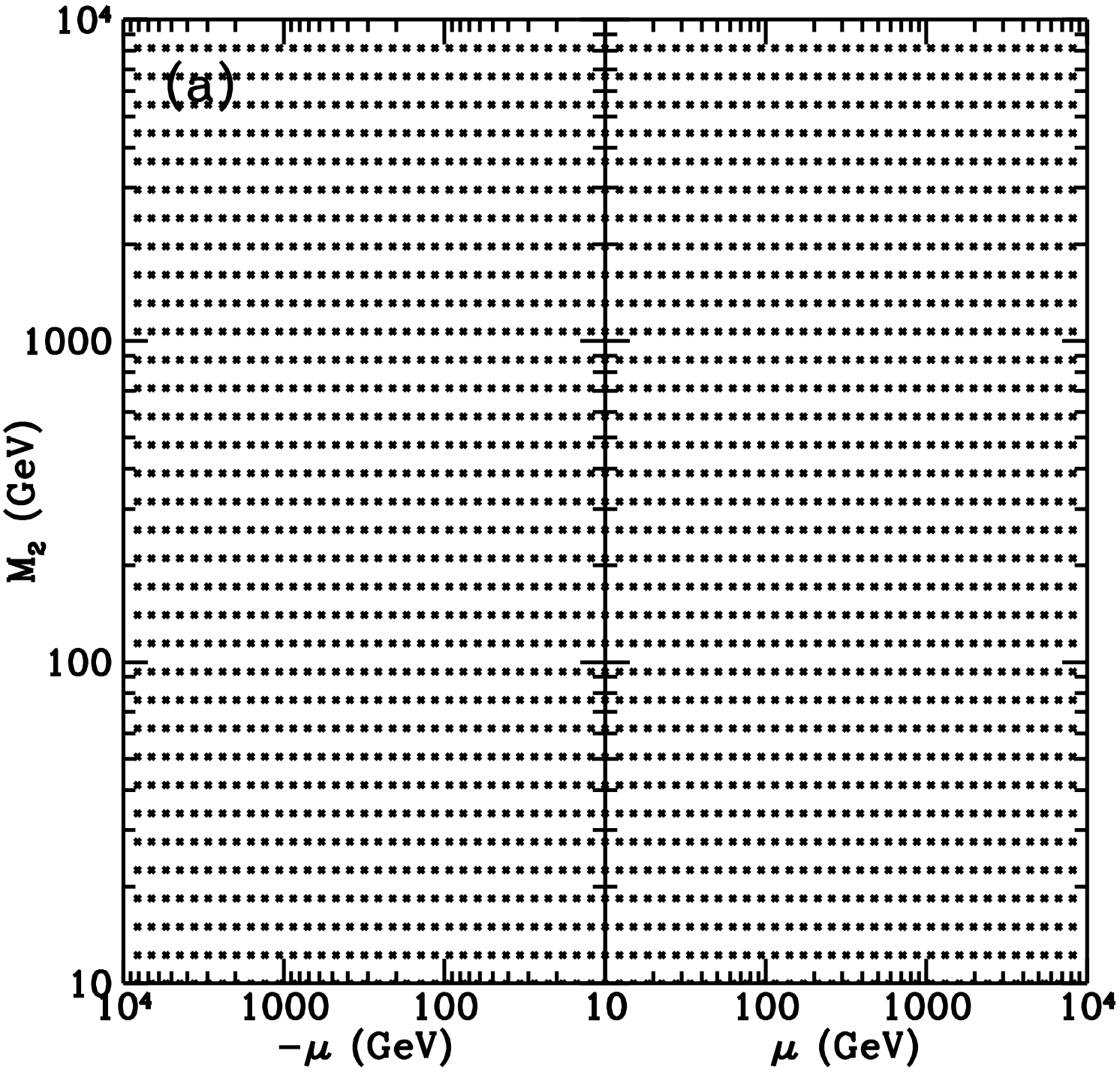
(a)
10^4
1000
100
10
M_2 (GeV)
10^4
1000
100
10
100
1000
10^4
$-\mu$ (GeV)
μ (GeV)

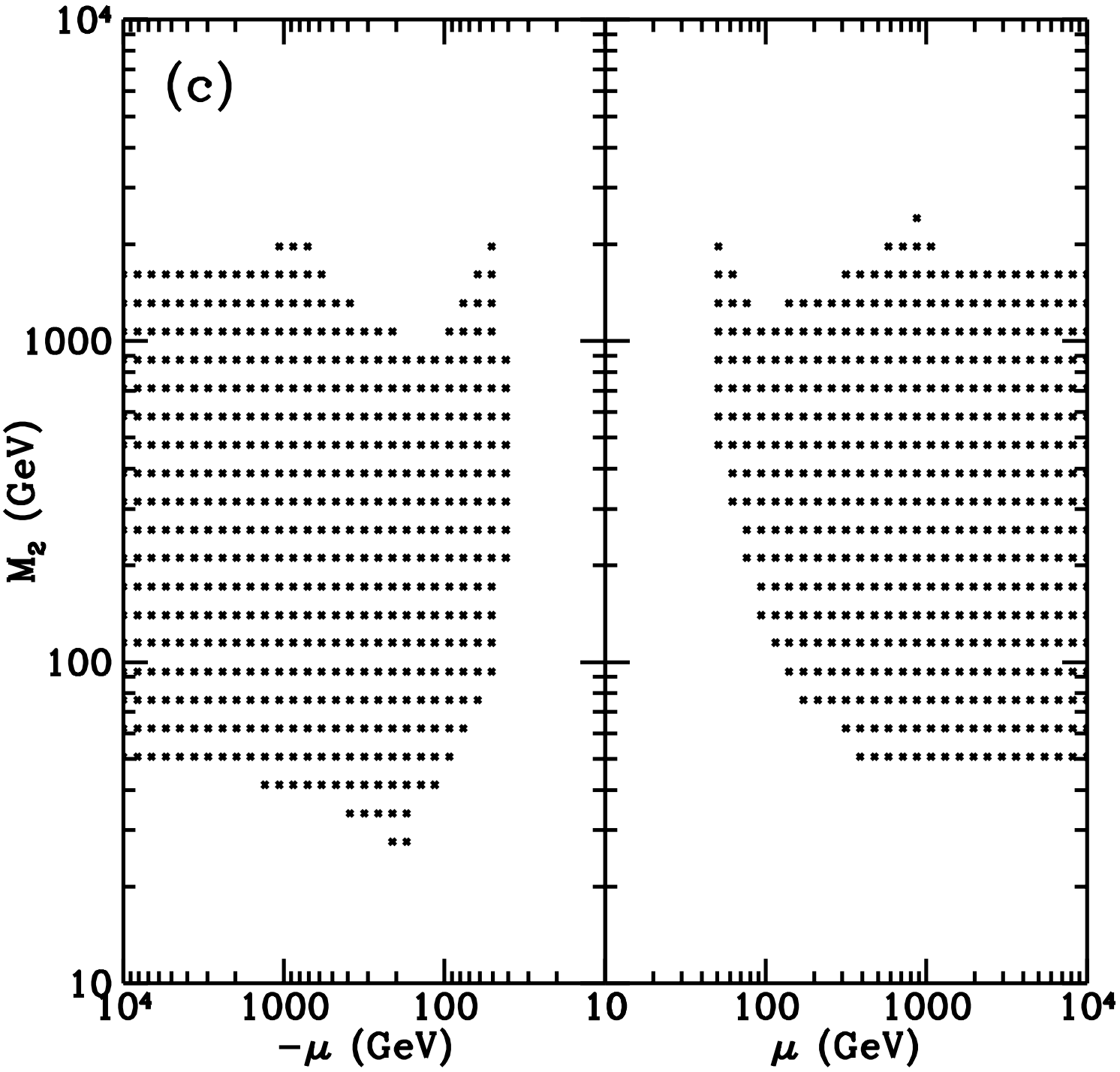
(c)
10^4
1000
100
10
M_2 (GeV)
10^4
1000
100
10
$-\mu$ (GeV)
10
100
1000
10^4
μ (GeV)

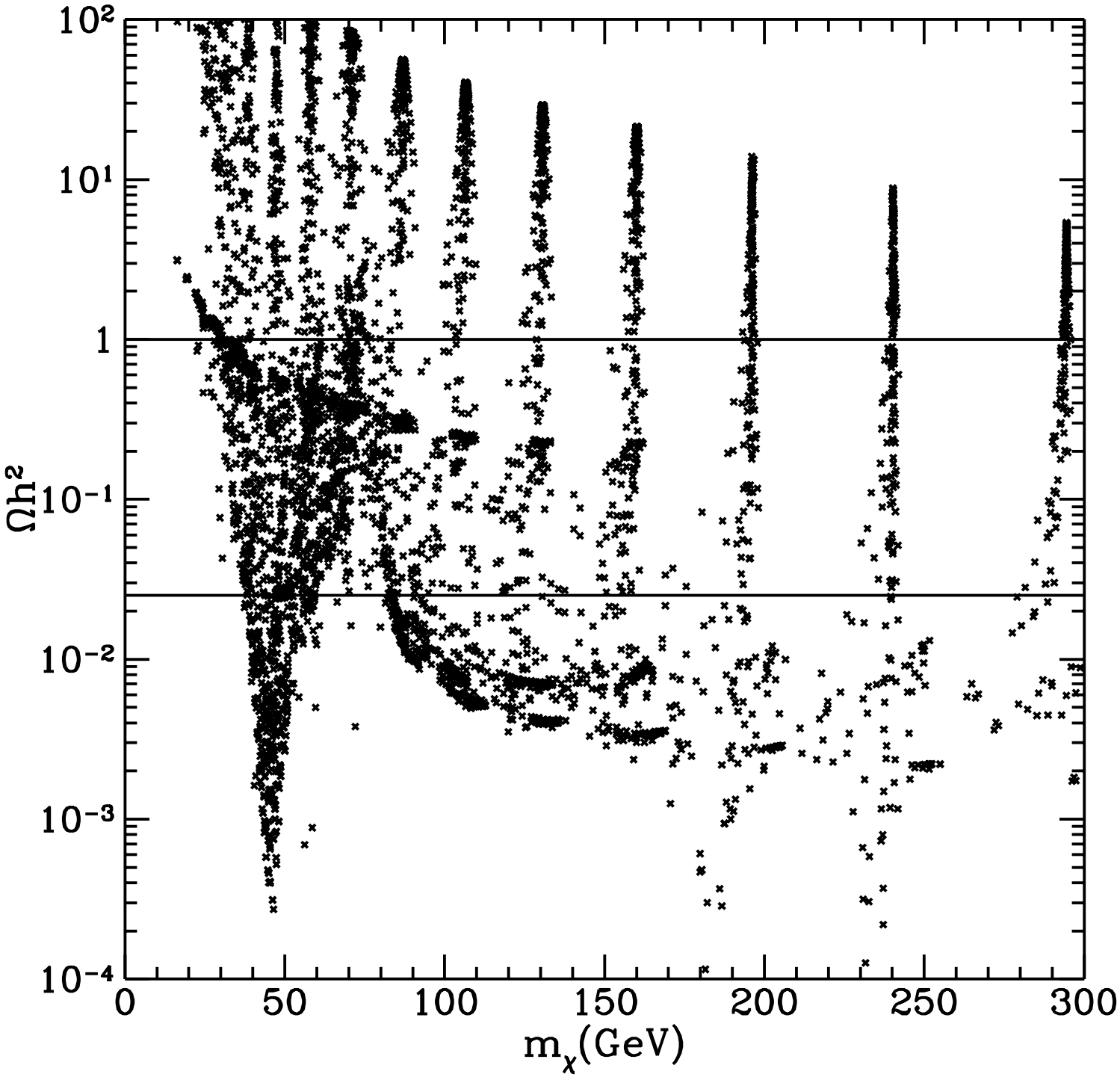
10^2
10^1
1
10^{-1}
10^{-2}
10^{-3}
10^{-4}
Ωh^2
0
50
100
150
200
250
300
m_χ(GeV)

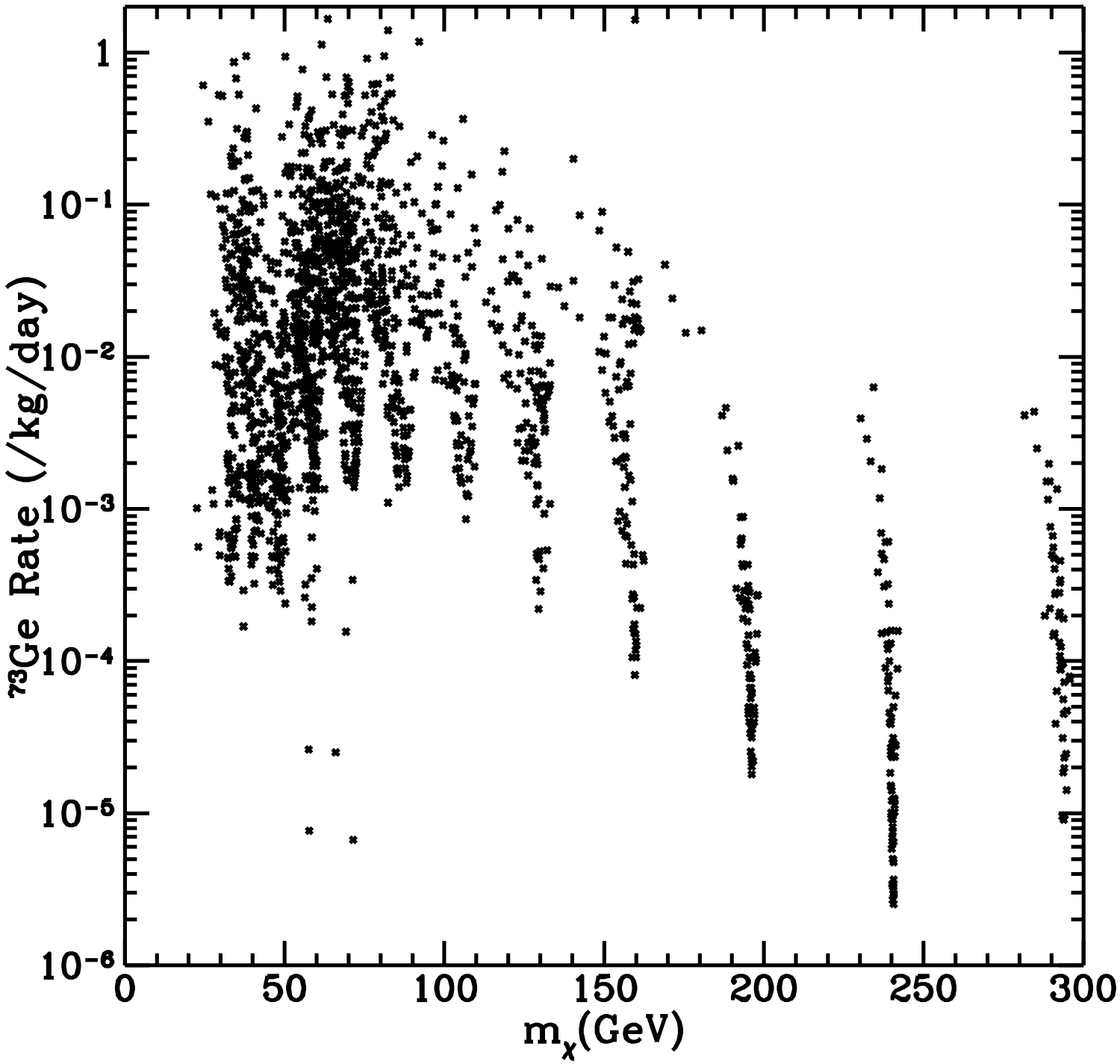
1
10^{-1}
10^{-2}
10^{-3}
10^{-4}
10^{-5}
10^{-6}
^{73}Ge Rate (/kg/day)
0
50
100
150
200
250
300
m_χ(GeV)

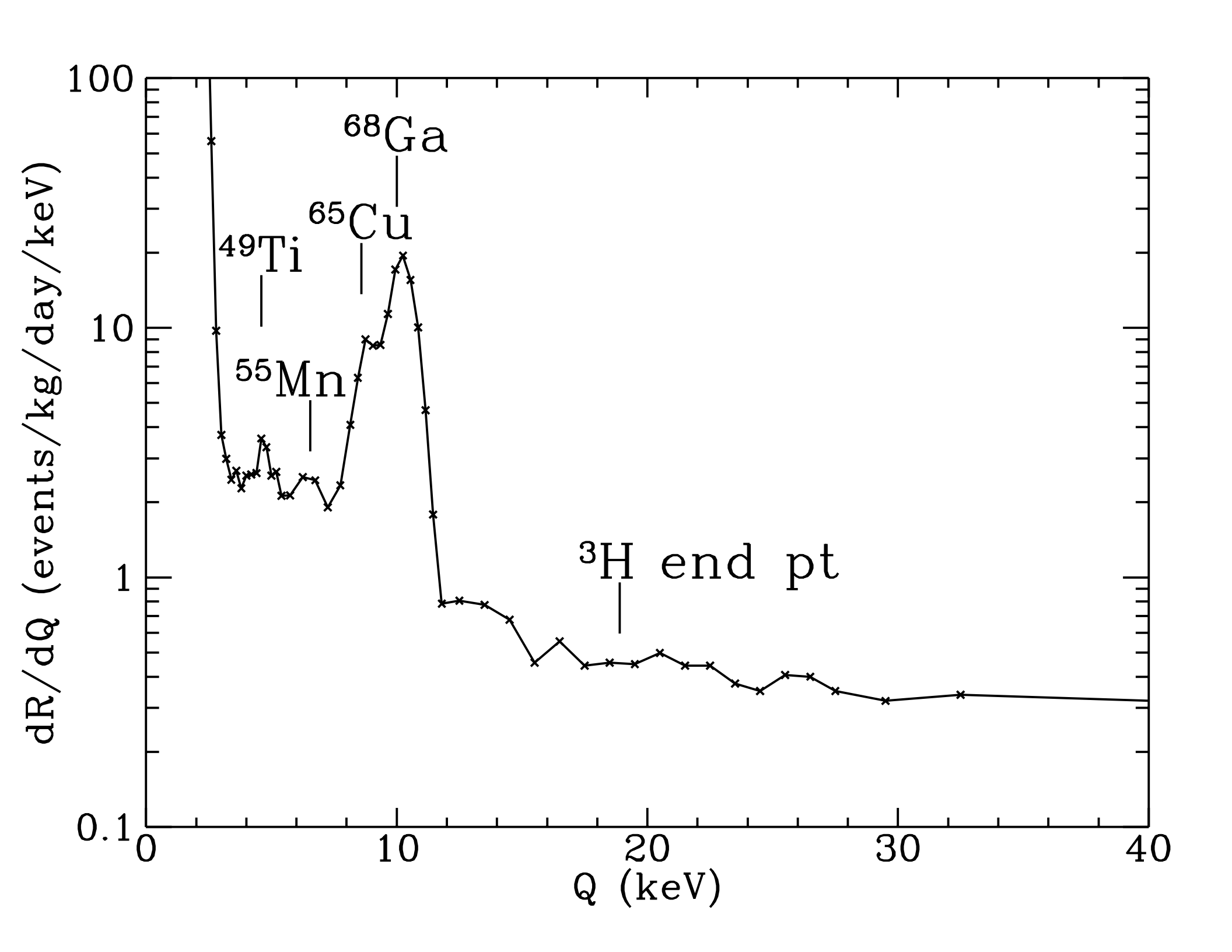
100
10
1
0.1
dR/dQ (events/kg/day/keV)
0
10
20
30
40
Q (keV)
^{68}Ga
^{65}Cu
^{49}Ti
^{55}Mn
^{3}H end pt

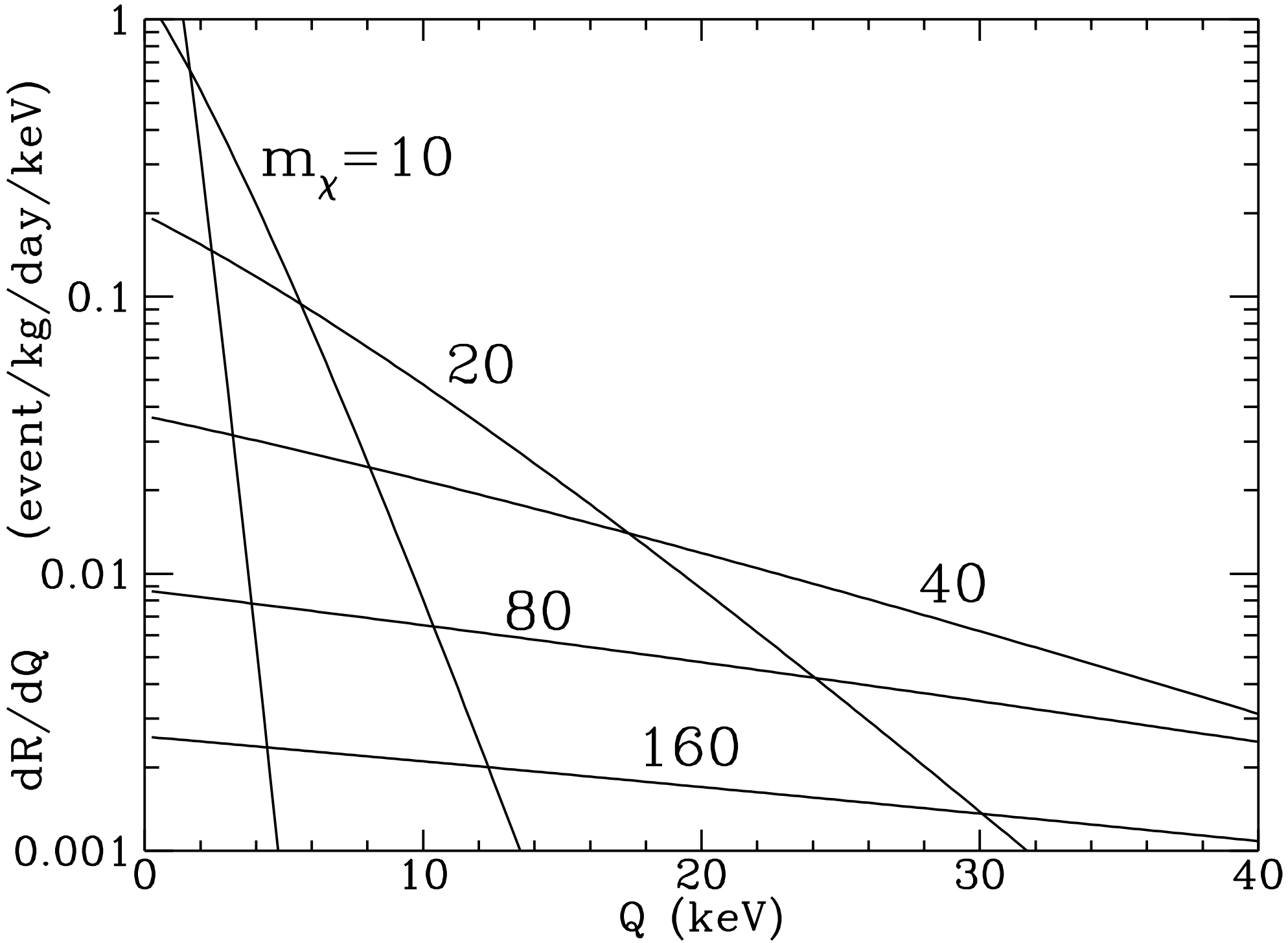
1
0.1
0.01
0.001
dR/dQ (event/kg/day/keV)
0
10
20
30
40
Q (keV)
$m_\chi = 10$
20
40
80
160

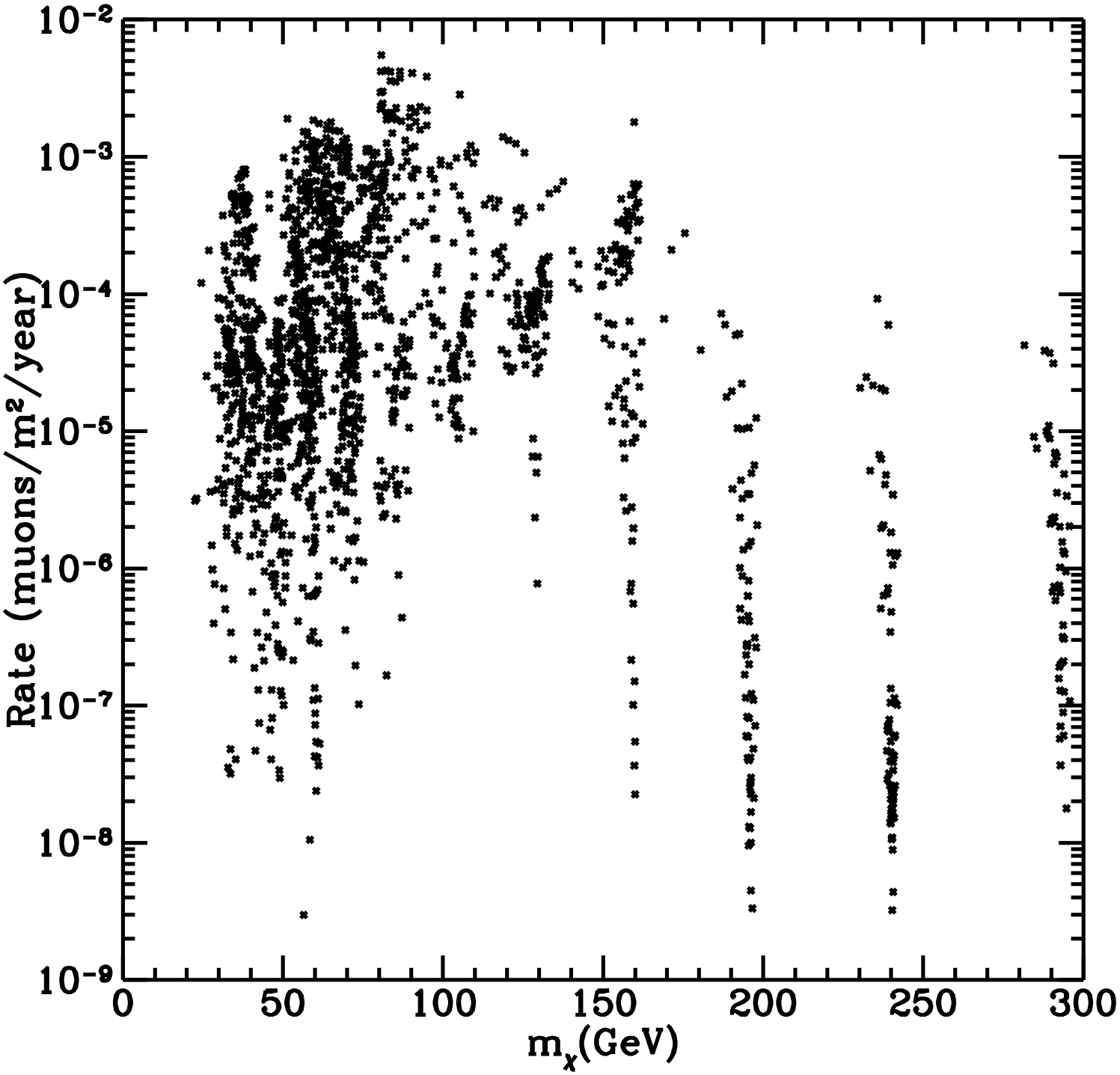
Rate (muons/m²/year)
10⁻²
10⁻³
10⁻⁴
10⁻⁵
10⁻⁶
10⁻⁷
10⁻⁸
10⁻⁹
0
50
100
150
200
250
300
m_χ(GeV)

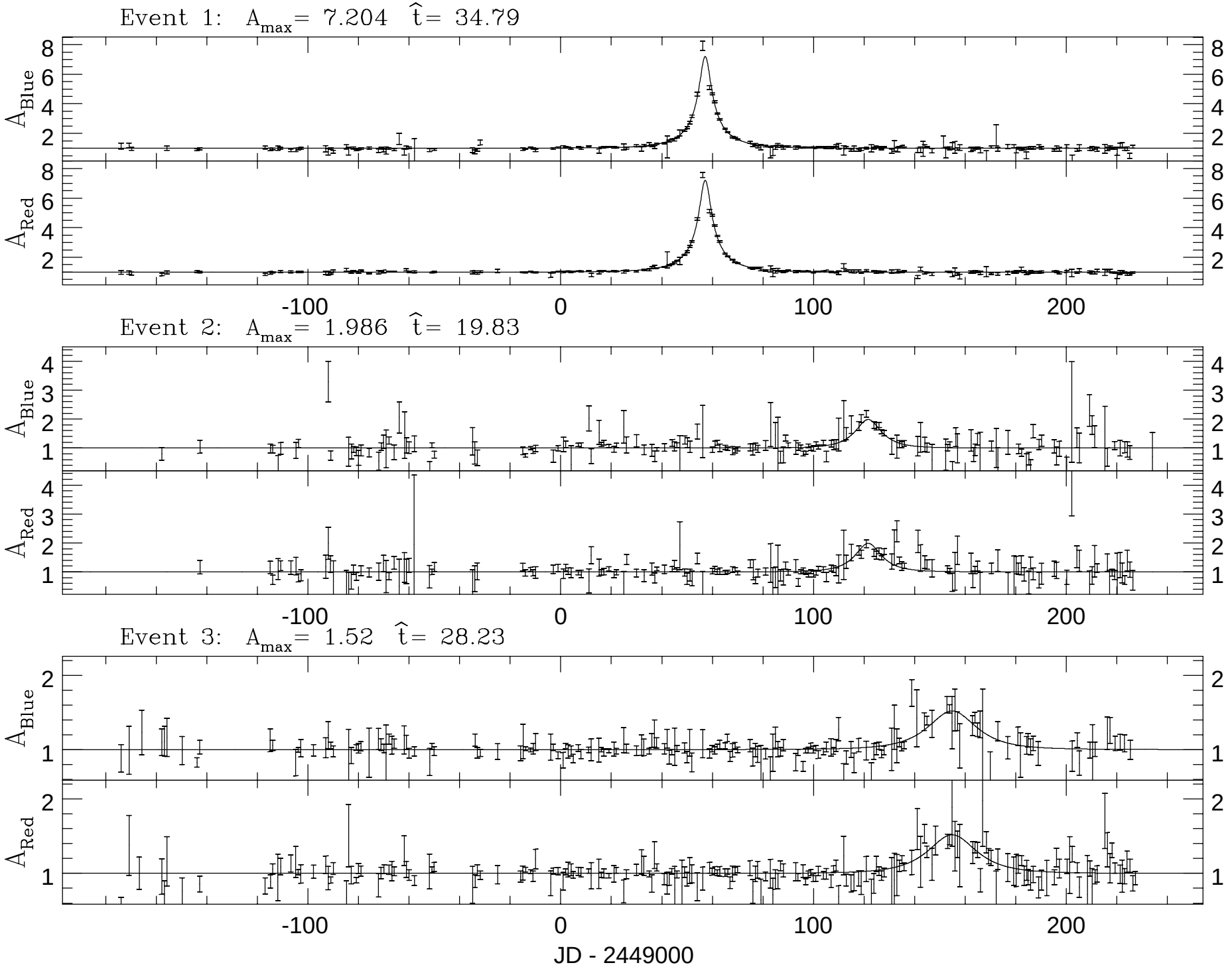
Event 1: A_{max}= 7.204 $\hat{t}$= 34.79
A_{Blue}
A_{Red}
Event 2: A_{max}= 1.986 $\hat{t}$= 19.83
A_{Blue}
A_{Red}
Event 3: A_{max}= 1.52 $\hat{t}$= 28.23
A_{Blue}
A_{Red}
-100
0
100
200
JD - 2449000

580/21, tile=108054 seq=75910 Rmag=18.8396 Vmag=19.7225
Amax=17.39 that=21.92 chi2dof=0.8887 pchi2dof=1.848 delchi2=1.727e+04

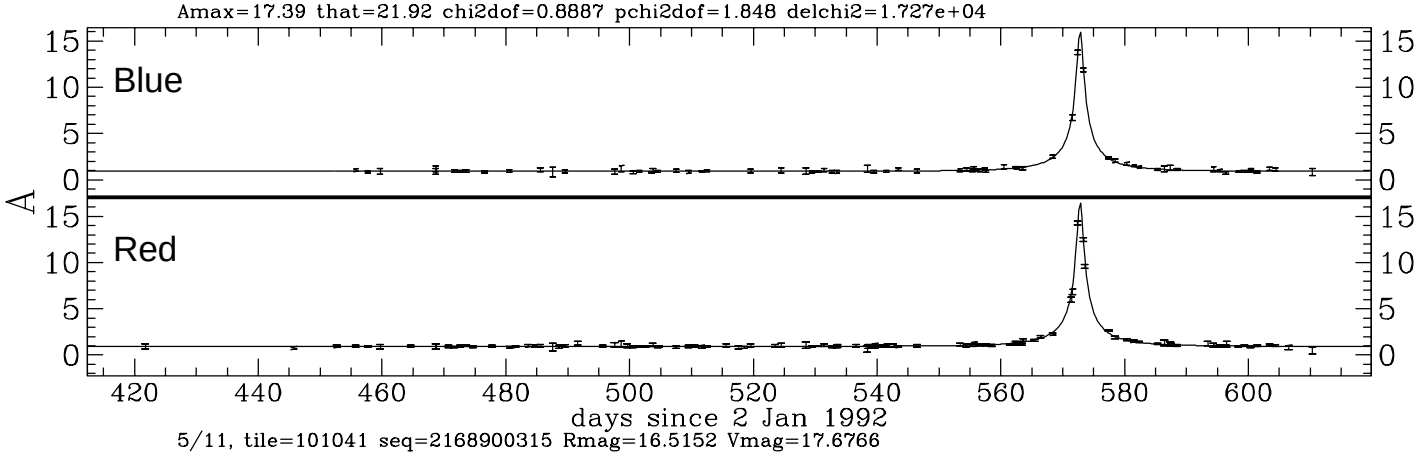

5/11, tile=101041 seq=2168900315 Rmag=16.5152 Vmag=17.6766
Amax=4.606 that=151.7 chi2dof=0.925 pchi2dof=0.9204 delchi2=8.834e+04

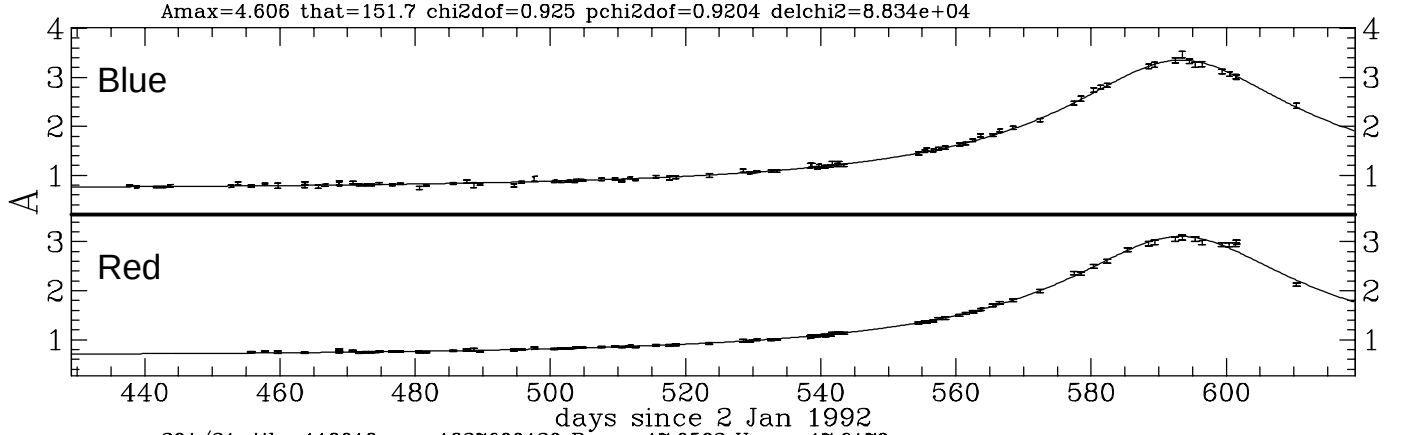

291/21, tile=118018 seq=1827600129 Rmag=17.0592 Vmag=17.6179
Amax=4.055 that=14.44 chi2dof=1.034 pchi2dof=1.336 delchi2=2.73e+04

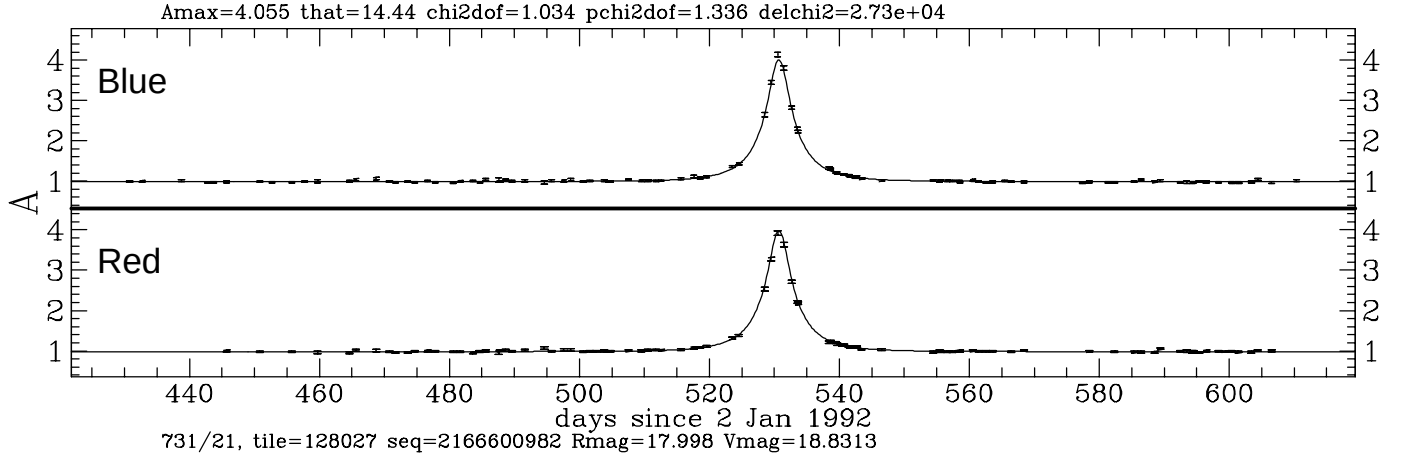

731/21, tile=128027 seq=2166600982 Rmag=17.998 Vmag=18.8313
Amax=7.115 that=16.38 chi2dof=1.686 pchi2dof=2.909 delchi2=3.158e+04

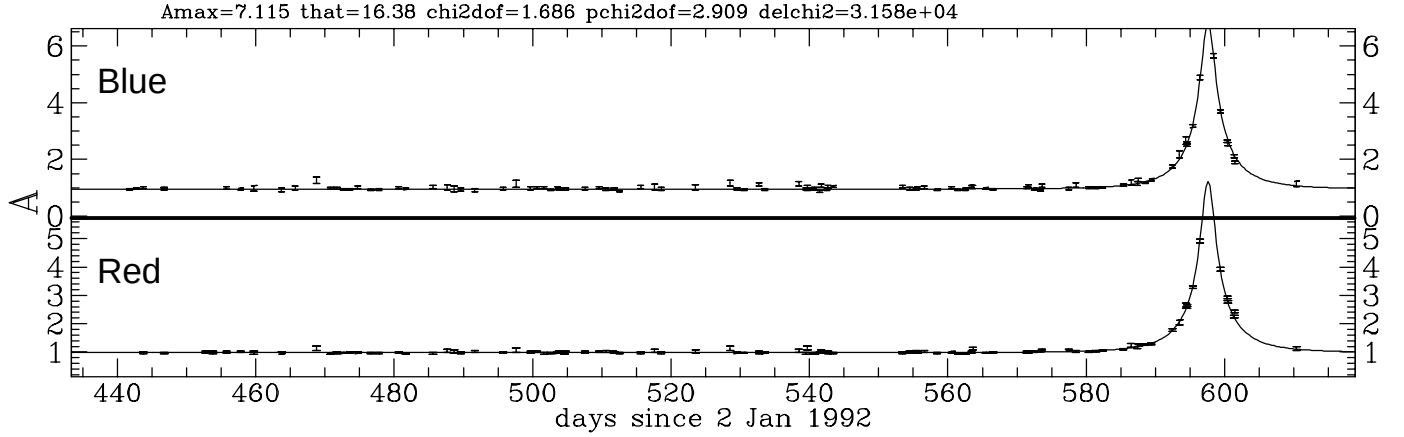

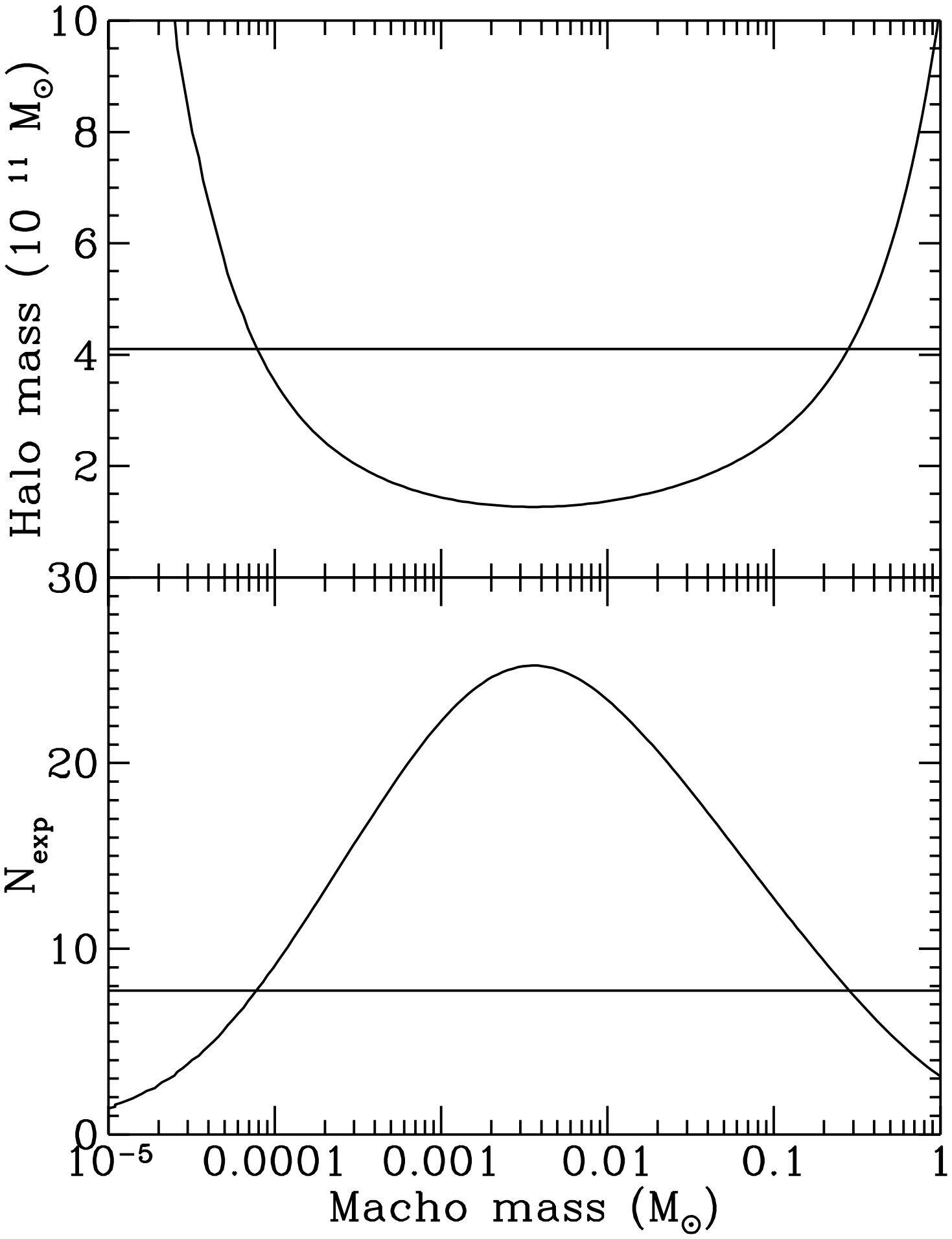
10
8
6
4
2
30
Halo mass (10^{11} $M_\odot$)
20
10
0
N_{exp}
10^{-5}
0.0001
0.001
0.01
0.1
1
Macho mass ($M_\odot$)